Received: 5 July 2023 | Revised: 18 October 2023 | Accepted: 18 October 2023

DOI: 10.1111/gcb.17050

Global Change Biology WILEY

RESEARCH ARTICLE

High methane concentrations in tidal salt marsh soils: Where does the methane go?

Margaret Capooci[1] | Angelia L. Seyfferth[1] | Craig Tobias[2] | Andrew S. Wozniak[3] | Alexandra Hedgpeth[4,5] | Malique Bowen[3] | Jennifer F. Biddle[3] | Karis J. McFarlane[5] | Rodrigo Vargas[1]

[1]Department of Plant and Soil Science, University of Delaware, Newark, Delaware, USA

[2]Department of Marine Sciences, University of Connecticut, Groton, Connecticut, USA

[3]School of Marine Science and Policy, University of Delaware, Lewes, Delaware, USA

[4]Department of Geography, University of California, Los Angeles, Los Angeles, California, USA

[5]Center for Accelerator Mass Spectrometry, Lawrence Livermore National Laboratory, Livermore, California, USA

Correspondence
Rodrigo Vargas, Department of Plant and Soil Science, University of Delaware, Newark, DE, USA.
Email: rvargas@udel.edu

Funding information
Division of Environmental Biology, Grant/Award Number: NSF-1247394 and NSF-1652594; U.S. Department of Energy, Grant/Award Number: DE-AC52-07NA27344, DE-SC0022185 and DE-SC0023099

Abstract

Tidal salt marshes produce and emit CH_4. Therefore, it is critical to understand the biogeochemical controls that regulate CH_4 spatial and temporal dynamics in wetlands. The prevailing paradigm assumes that acetoclastic methanogenesis is the dominant pathway for CH_4 production, and higher salinity concentrations inhibit CH_4 production in salt marshes. Recent evidence shows that CH_4 is produced within salt marshes via methylotrophic methanogenesis, a process not inhibited by sulfate reduction. To further explore this conundrum, we performed measurements of soil–atmosphere CH_4 and CO_2 fluxes coupled with depth profiles of soil CH_4 and CO_2 pore water gas concentrations, stable and radioisotopes, pore water chemistry, and microbial community composition to assess CH_4 production and fate within a temperate tidal salt marsh. We found unexpectedly high CH_4 concentrations up to 145,000 $\mu mol\,mol^{-1}$ positively correlated with S^{2-} (salinity range: 6.6–14.5 ppt). Despite large CH_4 production within the soil, soil–atmosphere CH_4 fluxes were low but with higher emissions and extreme variability during plant senescence ($84.3 \pm 684.4\,nmol\,m^{-2}\,s^{-1}$). CH_4 and CO_2 within the soil pore water were produced from young carbon, with most $\Delta^{14}C\text{-}CH_4$ and $\Delta^{14}C\text{-}CO_2$ values at or above modern. We found evidence that CH_4 within soils was produced by methylotrophic and hydrogenotrophic methanogenesis. Several pathways exist after CH_4 is produced, including diffusion into the atmosphere, CH_4 oxidation, and lateral export to adjacent tidal creeks; the latter being the most likely dominant flux. Our findings demonstrate that CH_4 production and fluxes are biogeochemically heterogeneous, with multiple processes and pathways that can co-occur and vary in importance over the year. This study highlights the potential for high CH_4 production, the need to understand the underlying biogeochemical controls, and the challenges of evaluating CH_4 budgets and blue carbon in salt marshes.

KEYWORDS
blue carbon, carbon cycling, fluxes, methane, radiocarbon, salt marsh

1 | INTRODUCTION

Information about methane (CH_4) dynamics in salt marshes lags behind CH_4 dynamics in freshwater wetlands, where emissions are usually high and affect the global carbon budget (Saunois et al., 2020). The prevailing paradigm of salt marsh carbon dynamics assumes limited CH_4 production due to high salinity and sulfate concentrations combined with reducing conditions, which promotes sulfate reduction. Studies show that salinity negatively correlates with soil–atmosphere CH_4 fluxes in salt marshes, with higher emissions at lower salinities (Al-Haj & Fulweiler, 2020; Poffenbarger et al., 2011). High sulfate concentrations in salt marsh soils are thought to contribute to low CH_4 emissions because sulfate-reducing bacteria outcompete hydrogenotrophic and acetoclastic methanogens (Mer & Le Roger, 2001) for substrates such as H_2, CO_2, and acetate (Ponnamperuma, 1972), thereby suppressing methanogenesis until sulfate levels have been depleted (King & Wiebe, 1980). However, sulfate-reducing bacteria do not affect the activity of methylotrophic methanogens, which could be important in salt marshes (Seyfferth et al., 2020). Recently, there has been recognition of the importance of CH_4 dynamics in salt marshes and other coastal ecosystems (i.e., mangroves, seagrasses), which complicates accounting protocols for "blue carbon" and brings attention to the underlying controls of CH_4 dynamics in these ecosystems (Capooci et al., 2019; Capooci & Vargas 2022b; Fettrow et al., 2023; Rosentreter et al., 2021; Windham-Myers et al., 2022).

The coastal and open ocean, including salt marshes, releases about 4–10 Tg CH_4 $year^{-1}$ (Saunois et al., 2020), but large uncertainties exist in CH_4 dynamics from coastal ecosystems. These uncertainties are propagated when representing terrestrial-aquatic interfaces in Earth System Models, where there is insufficient data regarding methanogenic biogeochemical pathways and the processes that dictate spatiotemporal variability in CH_4 dynamics (Ward et al., 2020). Concurrently, there has been increased interest in "blue carbon" ecosystems for their ability to store carbon (Nellemann et al., 2009), but there is uncertainty about whether greenhouse gas emissions from these ecosystems offset their carbon storage capabilities. For example, there is evidence that some salt marshes and mangroves emit enough CH_4 to offset their net carbon sequestration potential (Al-Haj & Fulweiler, 2020; Vázquez-Lule & Vargas, 2021), while other marshes, mangroves, and seagrass beds are net annual carbon sinks (Oreska et al., 2020; Rosentreter et al., 2018; Taillardat et al., 2020). Until there is a better understanding of CH_4 dynamics in coastal ecosystems and how the net balance between sources and sink changes, it will be difficult to assess their role as natural climate solutions for mitigating climate change (Macreadie et al., 2021).

Two scientific discoveries challenged the current paradigm surrounding salt marsh CH_4 production. First, a synthesis study found that CH_4 fluxes from coastal ecosystems can range from net uptake (−93 μmol m^{-2} day^{-1}) to net emission (94,000 μmol m^{-2} day^{-1}; Al-Haj & Fulweiler, 2020 and references within). The median CH_4 flux from salt marshes is low (~224 μmol m^{-2} day^{-1}; Al-Haj & Fulweiler, 2020), but the wide range of measured fluxes requires a closer look at the processes that control methanogenesis in these ecosystems. Second, the methylotrophic methanogenesis pathway is present in salt marsh and marine sediments (Seyfferth et al., 2020; Xiao et al., 2018; Zhuang et al., 2018). Methylotrophic methanogenesis uses non-competitive substrates such as methanol, methylsulfides, and methylamines, thereby enabling CH_4 production in the presence of sulfate reduction (Oremland et al., 1982; Xiao et al., 2018). Notably, *Spartina alterniflora*, a common salt marsh plant species, releases trimethylamine (TMA), a substrate for methylotrophic methanogenesis (Wang & Lee, 1994, 1995). Since CH_4 production in tidal salt marsh soils has long been thought to be dominated by hydrogenotrophic and acetoclastic methanogenesis, there is a need to revisit the paradigm and further explore CH_4 production and fate in salt marsh soils to improve modeling approaches across coastal ecosystems.

Salt marsh soils can contain large amounts of CH_4 (Seyfferth et al., 2020), but there remain questions about the production and age of CH_4 within the soil profile and its fate (e.g., lateral transport into tidal creeks, oxidation into CO_2). By answering these questions, we will better understand the conditions under which CH_4 is produced and which microbial pathways are important, whether CH_4 is stored in the soil or is rapidly turned over, and if it is not stored in the soil, where the CH_4 goes. Filling these knowledge gaps can inform process-based biogeochemical models, which could incorporate a better representation of CH_4 production, oxidation, and emission in wetland ecosystems (Oikawa et al., 2017; Zhang et al., 2002).

This study investigates the patterns and processes that govern CH_4 production, oxidation, and fluxes from soils in a temperate tidal salt marsh. We ask two interrelated questions. First, is it possible to have high CH_4 concentrations within the soil, and if so, are methylotrophic methanogens part of the soil microbial community? Due to evidence of high CH_4 concentrations at the site (Seyfferth et al., 2020), we hypothesized that methylotrophic methanogens might be present in soils, as well as contribute to CH_4 production, because the dominant plant community, *S. alterniflora*, is a source of non-competitive substrates used for methylotrophic methanogenesis (Wang & Lee, 1994, 1995). Second, what is the fate of the CH_4 within the soil profile? Soil CH_4 could persist in the soil, be transported vertically (e.g., degassing to the atmosphere) or laterally (i.e., advection from the marsh platform), or be oxidized into CO_2 and lost vertically as CO_2 or moved laterally as dissolved inorganic carbon (DIC). We hypothesized that the two most likely pathways for CH_4 loss are CH_4 oxidation, possibly contributing to high vertical CO_2 fluxes (Capooci & Vargas, 2022a, 2022b; Hill & Vargas, 2022; Vázquez-Lule & Vargas, 2021) and lateral transport to adjacent tidal creeks resulting in high CH_4 concentrations in surface water (Trifunovic et al., 2020). To answer these questions, we combined multiple approaches, including micrometeorological and isotope measurements, water chemistry, and microbial analyses. We present a combination of novel approaches and measurements, including radiocarbon dating of belowground CH_4 in a tidal salt marsh and evidence supporting methylotrophic methanogenesis as a relevant

metabolic pathway. These results provide evidence of high CH_4 production in salt marshes, raise concerns about current carbon accounting protocols, and provide new insights regarding carbon dynamics in these ecosystems.

2 | MATERIALS AND METHODS

2.1 | Study site and experimental setup

The study was conducted at St. Jones Reserve, a mesohaline tidal salt marsh in the Delaware National Estuarine Research Reserve (DNREC, 1999). The marsh is located within the Delaware Estuary and is tidally connected to the Delaware Bay via the St. Jones River. The study area has a complex biogeochemical heterogeneity, and there is evidence of simultaneous sulfate reduction and CH_4 production (Seyfferth et al., 2020). The experiment was performed in a short *S. alterniflora* [=*Sporobolus alterniflorus* (Loisel.); Peterson et al., 2014] dominated area referred to as "short *Spartina*" (i.e., SS) as established in previous studies (Capooci & Vargas, 2022a, 2022b; Seyfferth et al., 2020).

The SS experiences small daily tidal oscillations. The soil is nearly always saturated with small pockets of inundation at high tides. As a result, the pore waters are stagnant and redox potentials can reach −200 mV, particularly below 12 cm (Seyfferth et al., 2020). Above 12 cm depth, particularly from 0 to −7 cm, the diurnal tidal influence on water levels contributes to higher redox values, upwards of 200 mV (Seyfferth et al., 2020). Therefore, the site experiences strong redox gradients, ranging from oxic (0–7 cm depth) to anoxic (below ~10 cm depth).

The experiment comprised six campaigns during different canopy phenological stages. Canopy phenological stages have been identified as greenup (G), maturity (M), senescence (S), and dormancy (D) using Phenocams and standardized protocols at the study site (Hill et al., 2021; Trifunovic et al., 2020; Vázquez-Lule & Vargas, 2021). Briefly, for each day, an image from 12:00 h was selected, a region of interest was delineated to include only *S. alterniflora*, and the greenness index and phenophases were calculated using the phenopix R package (Filippa et al., 2020). The campaigns began during maturity (M) in the latter half of the year 2020 (M1—29 June to 2 July; M2—31 July to 3 August) followed by senescence (S1—31 August to 31 September, S2 to 28 September to 1 October). During the year 2021, two more campaigns were performed, one during dormancy (D1—22–26 March and 13–16 April) and another during greenup (G1—May 31 to June 3).

We used multiple methods and approaches to answer the questions posed in this study. First, we quantified the magnitudes and patterns of CH_4 and CO_2 soil-to-atmosphere fluxes and concentrations within the soil profile. Second, we collected gas, water, and soil samples for analyses of isotopes (i.e., $\delta^{13}C$ and $\Delta^{14}C$), water chemistry (e.g., salinity, sulfide, 3D excitation–emission matrix [EEM] spectroscopy), and microbial community composition. We collected CH_4 and CO_2 soil–atmosphere fluxes and concentrations, individual CH_4 and CO_2 samples, pore water samples, and soil samples during each campaign. The experiment could not start in either the late dormancy or greenup stage of 2020 due to the global lockdown during the beginning of the COVID-19 pandemic.

Our study focused on how CH_4 dynamics changed over time, where greenhouse gases and stable isotope fluxes were measured at multiple locations in space, but measurements that required sampling at different soil depths were performed at one location. Several reasons existed for the limited spatial replication of measurements across soil depths. One, the research was conducted in a designated protected area where we obtained permits from the state of Delaware to ensure minimal impact on the marsh ecosystem. These permits limited spatial replication of the study and could not be renewed or expanded during the COVID-19 pandemic. Two, the study was conducted during the COVID-19 pandemic, which required following the Centers for Disease Control and Prevention (CDC) guidelines that forced us to drastically reduce the personnel involved in the sampling campaigns and thus constrained the number of samples that could be feasibly collected. Three, some of our analyses, such as radiocarbon dating and microbial studies, are both financially demanding and time-intensive. Therefore, our options were constrained. While some of our findings do not capture spatial heterogeneity across the marsh, they agree with existing data collected at the site (Seyfferth et al., 2020). Overall, the results provide insights into the fate of CH_4 and pose additional questions that should be explored in future research.

2.2 | Concentrations and soil–atmosphere fluxes of CH_4 and CO_2

Depth profiles of soil CH_4 and CO_2 concentrations were measured using a passive gas sampler. Briefly, a frame was built to support gas-permeable silicone tubes (Seyfferth et al., 2020) that were placed horizontally within the frame to collect gases 15.5, 40, 56, and 70 cm below the soil surface. These depths were selected to be consistent with previous descriptions of the site's soil chemical and physical characteristics (Seyfferth et al., 2020). The sampler was installed in the summer of 2018 to allow for equilibration with the surrounding soil after the physical disturbance caused by the installation. CH_4 and CO_2 concentrations were measured using a non-dispersive infrared sensor (MH-Z92 Dual Gas CO_2/CH_4, CO_2 Meter; Ormond Beach, FL, USA) with a detection range of 0%–100% vol CH_4 and 0%–50% vol CO_2. This high-range instrument was chosen because prior analysis at the field site showed that concentrations of both gases exceeded 20,000 ppm and therefore saturated the detector of an Ultraportable Greenhouse Gas Analyzer (UGGA; Los Gatos Research, Santa Ana, CA, USA) (Seyfferth et al., 2020). At the start of each campaign (day 1), each silicone tube was filled with N_2 and then left to equilibrate for 5 days before measuring gas concentrations. On day 5, gas concentrations were measured by connecting the MH-Z92 sensor to a diaphragm pump and an in-line sampling port in a closed-loop,

along with a water trap and particulate filter. Gas concentrations are reported as the mean and standard deviation of a 1-minute timeframe when concentrations were steady.

Surface-atmosphere CH_4 and CO_2 fluxes were measured as described in Capooci and Vargas (2022b). Briefly, we installed six autochambers (LICOR 8100-104, Lincoln, NE, USA; volume: 4071.1 cm^3, Figure S1) on 20 cm diameter collars and connected a closed-path infrared gas analyzer (LI-8100A; LICOR) in parallel with a Fourier transform infrared spectrometer (DX4040; Gasmet Technologies Oy, Vantaa, Finland). Measurements were 5 min long and each chamber was measured once per hour over the course of an approximately 72-h campaign. Soil gas fluxes were calculated in SoilFluxPro, which uses both linear and exponential equations to calculate fluxes, (v4.2.1; LICOR) and underwent previously established QA/QC protocols to remove instrumental errors and flux values with an $R^2 < .90$ (Capooci et al., 2019; Capooci & Vargas, 2022b; Petrakis, Barba, et al., 2017; Petrakis, Seyfferth, et al., 2017).

2.3 | Radiocarbon and stable isotope measurements

Belowground CH_4 and CO_2, as well as soil–atmosphere CO_2 fluxes were collected for both stable ($\delta^{13}C$) and radiocarbon ($\Delta^{14}C$) isotope measurements during low tide. Soil–atmosphere CH_4 fluxes were collected for $\delta^{13}C$ measurements during low tide, but the fluxes were too low for $\Delta^{14}C$ analyses (minimum 20 μg C needed for analysis). Belowground CH_4 and CO_2 gas samples were collected in conjunction with measuring belowground CH_4 and CO_2 concentrations (see Section 2.2). After belowground concentrations were measured on day 5, an air-tight syringe was used to extract gas from each depth using the in-line sampling port. Gas samples designated for $\Delta^{14}C$ analyses were injected into a pre-evacuated serum vial capped with a septum, while samples for $\delta^{13}C$ were injected into N_2-filled exetainers.

Four 15-cm diameter soil collars were used to collect CH_4 and CO_2 gas emitted from the soil surface for $\delta^{13}C$ analyses. We placed a chamber connected in a closed-loop to an UGGA and outfitted it with a fan and an in-line sampling port. Samples were taken from the in-line port using a gas-tight syringe at 0, 5, 10, and 15 min after chamber closure. Gas samples were injected into N_2-filled exetainers, and the process was repeated for the remaining three collars. All stable isotope analyses ($\delta^{13}C$-CO_2, $\delta^{13}C$-CH_4) for gas samples were performed at the University of California-Davis Stable Isotope Facility using a ThermoScientific Delta V Plus isotope ratio mass spectrometer (IRMS).

The same set of collars used to collect $\delta^{13}C$ samples were used to collect $\Delta^{14}C$ samples. The three collars with the highest fluxes were used to collect samples to ensure enough carbon for $\Delta^{14}C$ analyses. To collect CO_2 gas emitted from the soil surface for $\Delta^{14}C$, first a chamber outfitted with a fan, a soda lime trap, and two ball valves was connected to the UGGA to purge the headspace of CO_2. Then the ball valves were closed and the UGGA was disconnected to allow for CO_2 to accumulate in the headspace. Once enough CO_2 accumulated, the headspace was extracted via a flow controller and a water trap into a 1 L stainless steel flask. This process was repeated for two additional collars.

A 70 cm deep soil core was collected with a gouge auger during the S2 campaign and was sectioned into 5 cm increments for several analyses, including bulk soil $\Delta^{14}C$. Subsamples from each increment were wrapped in aluminum foil for $\Delta^{14}C$ analyses before being transported to the laboratory to be air-dried. Visible plant litter was removed prior to processing and analyses.

CH_4 and CO_2 samples were processed for $\Delta^{14}C$ analyses at the Center for Accelerator Mass Spectrometry (CAMS) at Lawrence Livermore National Laboratory. CH_4 samples were extracted from serum vials and injected into a 5 L gasbag filled with zero air before being introduced to a cryogenic extraction line based on Kittler et al. (2017) and Petrenko et al. (2008) and described by McNicol et al. (2020). Briefly, gas samples were introduced to the vacuum line at ambient pressure, cryogenically purified to remove water and CO_2, combusted into CO_2, and further cryogenically purified before being recovered in a glass tube. For CO_2 samples, a series of cryogenic traps were used to purify and isolate the CO_2 before being recovered. A *S. alterniflora* sample, used to approximate local atmospheric $\Delta^{14}C$, was processed with an acid–base–acid pretreatment prior to combustion. Soil samples were combusted in a sealed tube in the presence of CuO and Ag. Prior to graphitization, both plant and soil sample-derived CO_2 was split to measure $\delta^{13}C$ of the bulk soil and the plant sample. The splits were sent to the Stable Isotope Geosciences Facility at Texas A&M and were measured on a ThermoScientific MAT 253 Dual Inlet IRMS. All purified samples were then reduced to graphite onto Fe powder in the presence of H_2 (Vogel et al., 1984).

Graphite targets derived from gas samples were measured on the Van de Graaff FN Tandem Accelerator Mass Spectrometer (AMS), while graphite derived from soil and plant samples was measured on the NEC 1.0 MV Model 3SDH-1 Tandem AMS (Broek et al., 2021) at CAMS. Radiocarbon data are reported in $\Delta^{14}C$ notation and have been corrected for ^{14}C decay since 1950, the year of measurement (2020 or 2021), and for mass-dependent fractionation with measured $\delta^{13}C$ values (Stuiver & Polach, 1977). Error across all samples for both instruments was 3.3% ± 0.8‰.

2.4 | Interpreting radiocarbon data

Carbon has three isotopes, ^{12}C, ^{13}C, and ^{14}C, two of which are stable isotopes (^{12}C and ^{13}C) and one of which is a radioisotope (^{14}C). ^{14}C is continually produced in the upper atmosphere, where it oxidizes into $^{14}CO_2$ and gets distributed throughout atmospheric, terrestrial, and oceanic C reservoirs (Schuur et al., 2016). In the late 1950s and early 1960s, atmospheric levels of ^{14}C doubled due to atmospheric nuclear weapons testing (Manning & Melhuish, 1994). ^{14}C levels have been subsequently declining due to the ban on atmospheric nuclear weapons testing in 1963 and from fossil fuel

emissions (Graven et al., 2012; Levin & Hesshaimer, 2000). Due to these changes in ^{14}C concentrations, C has a ^{14}C signature unique to the year it is assimilated by plants. As such, ^{14}C measurements can give researchers an idea of the average age (or time since assimilation from the atmosphere) of a particular form of C. A $\Delta^{14}C$ value of 0 is assigned to 1950 by convention (Trumbore et al., 2016), with positive values indicating that the C in the sample was assimilated from the atmosphere after 1950 and includes "bomb" carbon. Likewise, negative $\Delta^{14}C$ values indicate the C in the sample was produced before 1950.

2.5 | Pore and surface water chemistry analyses

Pore water samples were collected using a PushPoint (M.H.E. Products) connected to a peristaltic pump via tubing with a needle at the outlet. Samples were pumped at low tide from 15.5, 40, 56, and 70 cm below the soil surface to align with the gas sampling depths and were collected in N_2-filled 60 mL glass serum vials capped with a septum. Surface water samples were also collected from the tidal creek at low and high tide, and from the nearby St. Jones River. All water samples were stored on ice until they could be transported to the laboratory to be aliquoted into transport tubes (salinity, sulfide) or filtered through a 0.2 µm syringe filter into PETG vials (dissolved organic carbon [DOC], DIC, EEMs, and ultraviolet–visible [UV–VIS]) in an anaerobic chamber. Sulfide and conductivity measurements were performed immediately, while DOC, DIC, EEMs, and UV–VIS samples were stored in the freezer (DOC, DIC) or in the refrigerator (EEMs, UV–VIS) until analysis.

Pore and surface water samples were measured for salinity and sulfide as described by Northrup et al. (2018). DOC concentrations were determined by high temperature catalytic oxidation using a Shimadzu TOC-VCPH Total Organic Analyzer (Sharp, 2002). DIC concentrations were calculated by subtracting DOC concentration from the total organic carbon (TOC) concentration, whereby TOC was measured on filtered, un-acidified samples with the Shimadzu TOC-VCPH Total Organic Analyzer. DOC and DIC standard errors are reported and were derived from multiple injections of the same sample.

Absorption and EEMs scans were measured on filtered samples using a Horiba Aqualog, which characterizes both colored and fluorescent dissolved organic matter (DOM) using absorption and fluorescence spectroscopy. Specific ultraviolet absorbance (SUVA) was calculated by dividing the UV absorbance of a sample at 254 nm by the DOC concentration (Chin et al., 1994; Weishaar et al., 2003). $SUVA_{254}$ is a measure of the aromaticity of chromophoric DOM (Chin et al., 1994; Weishaar et al., 2003). For EEMs, wavelengths were scanned from 230 to 700 nm in 2 nm increments. Data were corrected for inter-filter effects and normalized using the raman area method. Fluorescence index (FI) was calculated by taking the ratio of λ_{em} 470–520 nm at λ_{ex} of 370 nm (Cory & McKnight, 2005; McKnight et al., 2001). FI can be used to assess autochthonous versus allochthonous changes in DOM (Hood et al., 2005; Miller & McKnight, 2010), since terrestrially derived DOM tends to be enriched in high molecular weight components compared to microbially derived DOM (Romera-Castillo et al., 2014). For both $SUVA_{254}$ and FI, no replicates were run.

2.6 | Microbial community analyses

Samples from the soil core collected during S2 (described in Section 2.3) were placed in sterile vials for 16S rRNA sequencing and placed on ice for transport to the laboratory to be stored in a −80°C freezer until DNA extraction and sequencing. For DNA extraction, soil samples were homogenized with 100 mL of 1× PBS. DNA was extracted from all samples using the Qiagen DNeasy Power Soil Pro kit. The extracted DNA was sent to UCONN Core Sequencing facility for amplicon sequencing of the 16S rRNA gene in the V3–V4 region. After receiving forward and reverse sequences from UCONN, they were quality checked, and only the forward sequence reads were further processed. The forward sequence reads were processed using a MOTHUR pipeline (Schloss et al., 2009). Forward sequences were trimmed to 130–200 bp range, ambiguous nucleotides were removed, and then operational taxonomic units (OTUs) with a 3% dissimilarity were created. OTUs were then aligned and classified using the Silva138 database (Quast et al., 2013). Sequence data from this study are available in the National Center for Biotechnology Information under BioProject number PRJNA1019769.

2.7 | Data analyses

We report the mean and standard deviation for CH_4 and CO_2 fluxes, DOC, and DIC concentrations. Keeling plots were fitted with model II regression using the R package "lmodel2" (Legendre, 2018) to calculate the $\delta^{13}C\text{-}CH_4$ and $\delta^{13}C\text{-}CO_2$ of soil efflux (Pataki et al., 2003). The 95% confidence intervals associated with the regression were reported in Figure S2 and were calculated using a bootstrapping method. Selected microbial taxa associated with aerobic methane oxidation (e.g., *Methylobacter*, *Methylocystis*), anaerobic methane oxidation (*Methanomicrobia*), hydrogenotrophic methanogenesis (e.g., *Methanomicrobiales*, *Methanobacteriales*), methylotrophic methanogenesis (*Methanomassiliicoccales*, *Methanofastidiosa*), and sulfate reduction (*Desulfosarcina*) were identified and summed for each category (Table S1; Figures S3–S5).

3 | RESULTS

3.1 | Soil and pore water characteristics

We found very high levels of CH_4 concentrations in the soil profile up to ~145,000 µmol mol^{-1}, and CO_2 concentrations up to 500,000 µmol mol^{-1} (Figure 1a,b). CH_4 concentrations generally peaked at −56 cm and declined closer to the soil surface, but CO_2

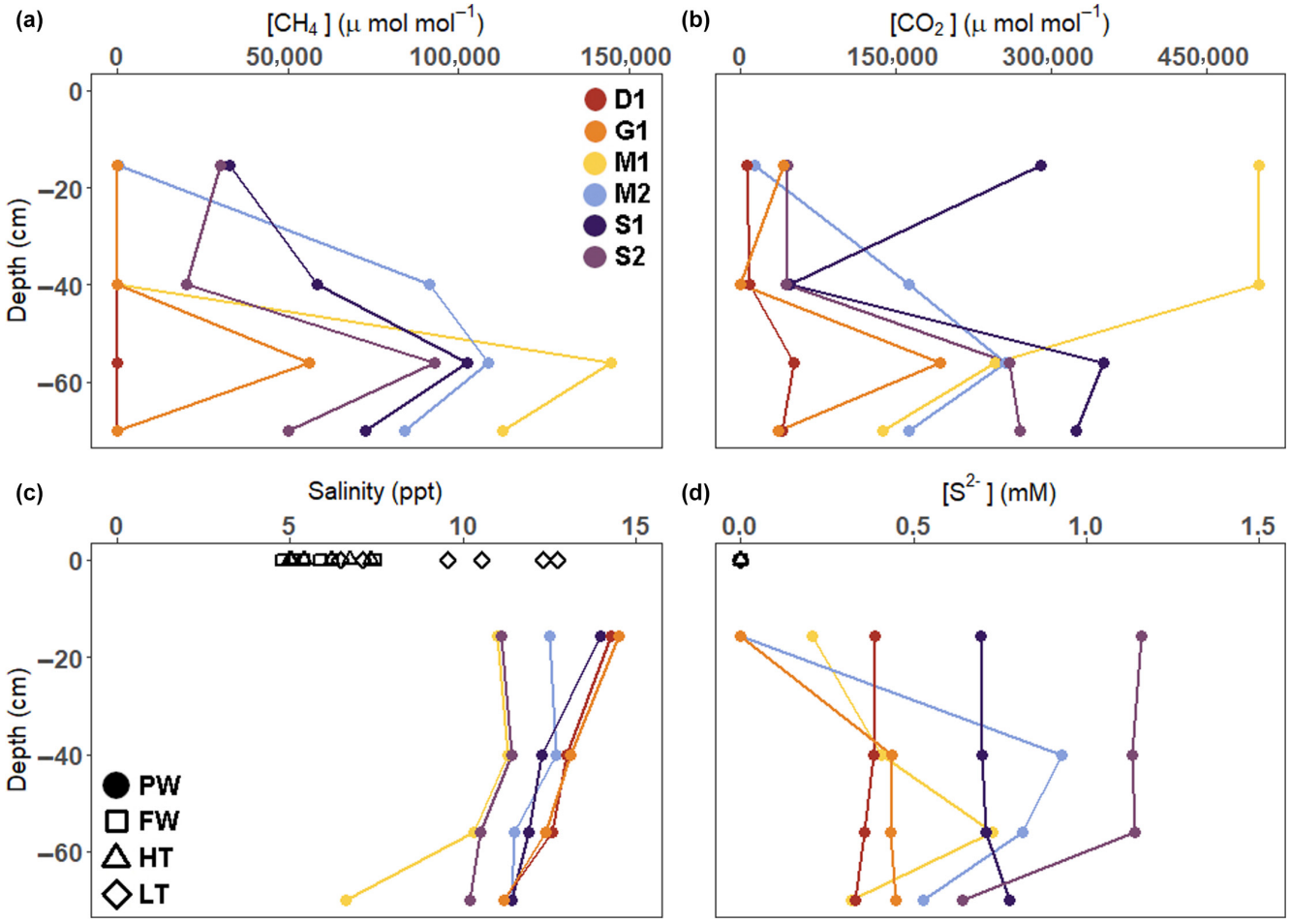

FIGURE 1 Depth profiles of pore water (a) CH_4 and (b) CO_2 concentrations, as well as pore water and surface water (c) salinity and (d) sulfide (S^{2-}) during each of the six campaigns. For water samples: FW, surface water at St. Jones River; HT, tidal creek at high tide; LT, tidal creek at low tide; PW, pore water at low tide. For phenophase: D, dormancy; G, greenup; M, maturity; S, senescence; 1: first campaign during a phenophase; 2: second campaign during a phenophase.

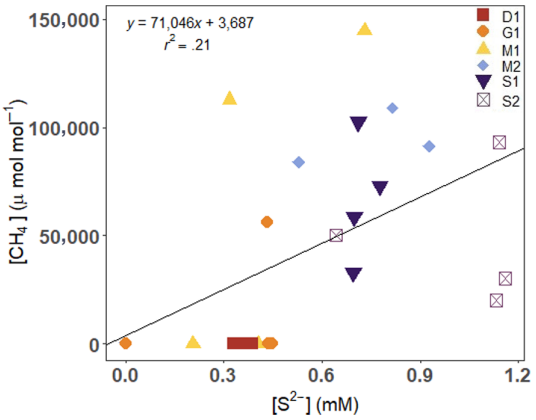

FIGURE 2 Relationship between pore water sulfide concentrations and mean soil CH_4 concentrations for all campaigns and all depths. The *p*-value of the slope is .01.

concentrations did not appear to have a consistent pattern with depth. Overall, soil gas concentrations were higher in the maturity and senescence canopy phenophases than in greenup and dormancy.

Pore water salinity ranged from 6.6 to 14.5 ppt and generally increased closer to the soil surface (Figure 1c). The pore water typically had higher salinity than the river and the tidal creek at high tide but was similar to the tidal creek's salinity at low tide. Sulfide was present in the soil pore water in concentrations ranging from 0 to 1.2 mM (Figure 1d) and was generally higher later in the growing season (Figure 1d). Sulfide was positively correlated with CH_4 concentration, illustrating that CH_4 concentrations increase even in the presence of sulfate reduction (Figure 2; *p*-value = .01; intercept standard error = 17,503; slope standard error = 26,869).

Mean soil–atmosphere CH_4 fluxes ranged from $21.8 \pm 12.8\,nmol\,m^{-2}\,s^{-1}$ during G1 to $84.3 \pm 684.4\,nmol\,m^{-2}\,s^{-1}$ during S2 (Figure 3a). The annual mean of CH_4 fluxes was $41.2 \pm 291.5\,nmol\,m^{-2}\,s^{-1}$. Soil–atmosphere CH_4 fluxes showed a seasonal pattern with higher fluxes (~23% to 105% higher than the annual mean) during S1 and S2 and lower fluxes during D1 and G1 (~36%–47% lower than the annual mean). Mean CO_2 fluxes ranged from $0.81 \pm 0.44\,\mu mol\,m^{-2}\,s^{-1}$ during D1 to $3.33 \pm 1.5\,\mu mol\,m^{-2}\,s^{-1}$ during G1 (Figure 3c). The annual mean of CO_2 fluxes was $1.92 \pm 1.3\,\mu mol\,m^{-2}\,s^{-1}$. CO_2 fluxes peaked earlier in the growing

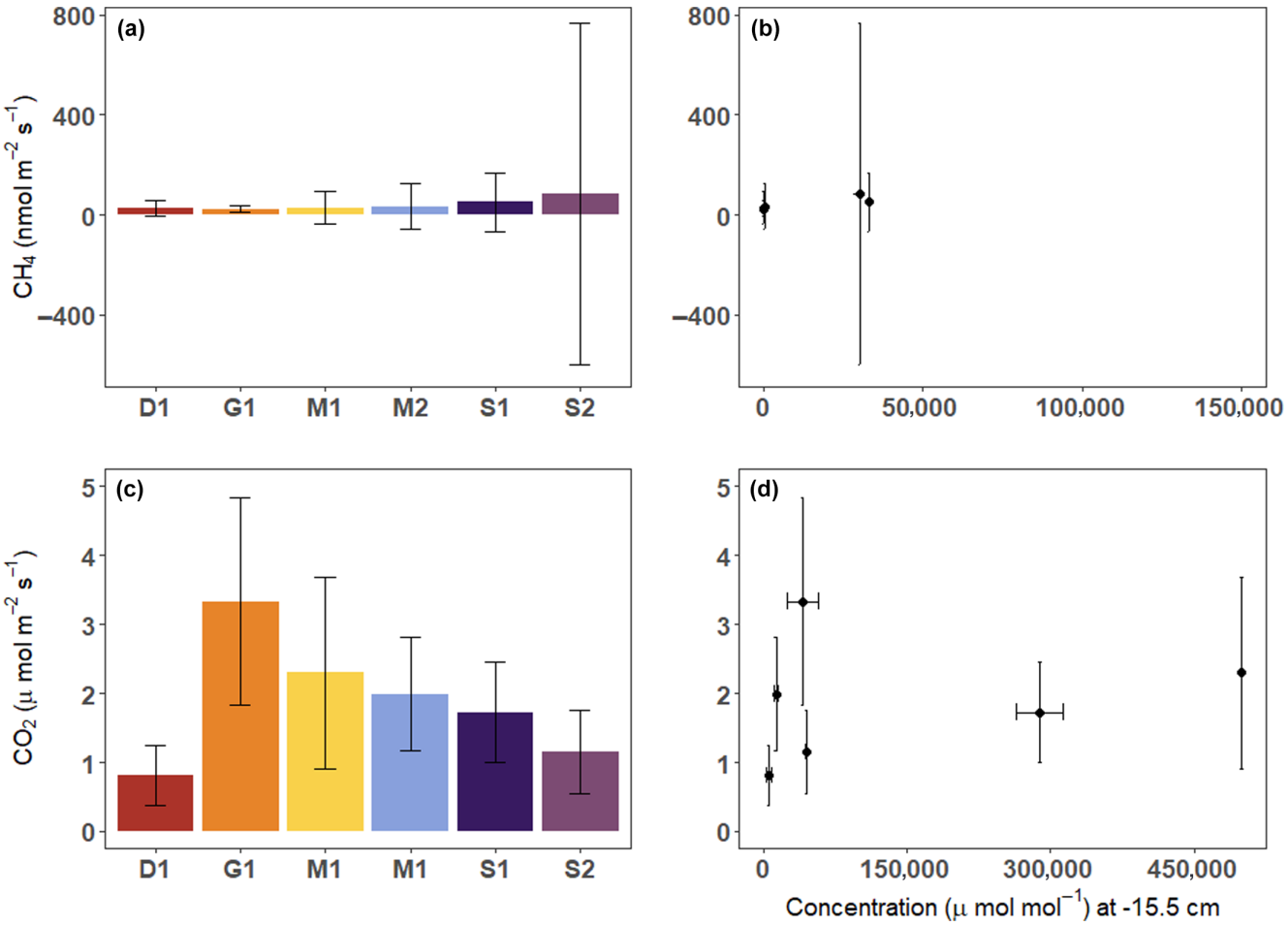

FIGURE 3 Mean ± SD of (a) CH_4 and (c) CO_2 soil–atmosphere fluxes during each campaign. Panels (b, d) show the relationship between the mean concentration of CH_4 and CO_2 at 15.5 cm depth compared to the corresponding mean soil–atmosphere flux for each campaign. Note that horizontal error bars for panels b and d are sometimes too small to be discernable.

season (G1) compared to CH_4 fluxes. When comparing the gas concentration nearest the surface (at −15.5 cm) to the soil–atmosphere fluxes, we found an apparent significant relationship for CH_4 ($p = .03$, $r^2 = .66$, $y = 0.001x + 28$) with higher gas concentrations near the soil surface corresponding to higher soil–atmosphere CH_4 fluxes (Figure 3b), which was not the case for CO_2 (Figure 3d).

3.2 | CH_4 and CO_2 stable isotopes and radiocarbon

The δ^{13}C-CH_4 within the soil ranged from −68.8‰ to −46.4‰ with similar trends with depth across the six campaigns (Figure 4a). Generally, the heaviest δ^{13}C-CH_4 during each campaign was located at −40 cm. The δ^{13}C-CH_4 from soil–atmosphere fluxes had a broader range of values from −80.1‰ to −17.7‰ but were generally between −60‰ and −40‰ (Figure 4a). The δ^{13}C-CO_2 for both the depth profiles and the soil surface fluxes were heavier than the corresponding δ^{13}C-CH_4 values. Depth profiles of δ^{13}C-CO_2 had little variation and ranged from −19.6‰ to −12.2‰ (Figure 4b). The δ^{13}C-CO_2 from the soil–atmosphere flux had a broader range from −31.0‰ to −2.4‰. There was no significant relationship between δ^{13}C-CH_4 and δ^{13}C-CO_2 (Figure 4c) for both soil–atmosphere fluxes and concentrations.

The depth profiles of Δ^{14}C-CH_4 show that CH_4 within the soil is usually modern or recently produced (Figure 5a), particularly during S2 where CH_4 had values between +53‰ and +66‰. However, we did find older CH_4 within the soil profile with Δ^{14}C as low as −517‰. Similarly, Δ^{14}C-CO_2 depth profiles showed that CO_2 within the soil is modern or recently produced, with some older CO_2 ($\Delta^{14}C = -156$‰) (Figure 5b). Soil–atmosphere CO_2 fluxes had modern or recently produced CO_2, but were generally slightly older than the CO_2 within the soil profile (Figure 5b). The oldest soil–atmosphere CO_2 flux had a value of −161‰. For both soil–atmosphere fluxes and concentrations of CO_2, Δ^{14}C-CO_2 during greenup and maturity was slightly older than during senescence. We found no significant relationship between the age of CH_4 concentrations and the age of CO_2 concentrations at corresponding depths and time points (Figure 5c). We also measured the bulk soil Δ^{14}C, which ranged from +218‰ to −111‰, with a profile that captured the atmospheric Δ^{14}C bomb curve.

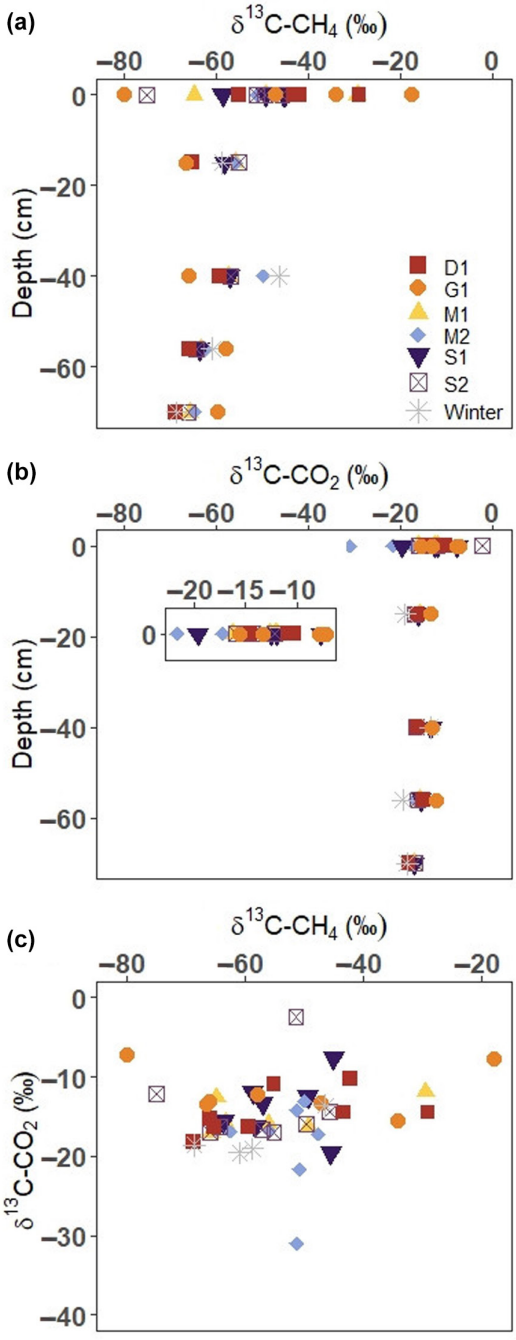

FIGURE 4 Plots showing (a) δ^{13}C-CH_4 and (b) δ^{13}C-CO_2 of the depth profiles and the soil surface fluxes, as well as (c) the relationship between δ^{13}C-CH_4 and δ^{13}C-CO_2. Data at 0 cm in plots (a, b) represent soil surface fluxes to the atmosphere. Plot (b) inset shows the δ^{13}C-CO_2 of the soil flux. The winter profile represents the isotopic values of CO_2 and CH_4 between the 28 September–1 October 2020 and the 22–26 March sampling events when the passive gas sampler was left to equilibrate over the winter.

3.3 | Surface and pore water carbon chemistry

Surface water DOC concentrations ranged from 0.40 to 1.06 mM with the highest concentrations within the tidal creek during low tide (Figure 6a). Pore water DOC concentrations were, on average, ~200% higher than the surface waters, ranging from 1.28 to 3.09 mM. The highest concentrations occurred earlier in the growing season (G1, M1), while the lowest occurred during D1 and S1. Similar to DOC, surface water DIC concentrations were lower than the pore water, ranging from 1.99 to 5.33 mM (Figure 6b). Pore water DIC ranged from 11.5 to 29.1 mM. There is a seasonal progression in the DIC concentrations, with the lowest values found during S1, increasing in S2, and peaking during D1, after which the concentrations decreased through greenup (G1), maturity (M1, M2), and early senescence (S1).

We also analyzed $SUVA_{254}$ and FI, which are indicators of how processed the carbon is and whether the carbon is more terrestrially derived versus microbially derived. $SUVA_{254}$ is lower in the surface waters compared to the soil pore waters (Figure 6c). Surface water $SUVA_{254}$ ranged from 2.40 to 3.91, while soil pore water ranged from 3.68 to 19.2. The highest values occurred during D1 and M2, while the lowest occurred during G1 and M1. FI values in the surface waters ranged from 1.17 to 1.28, while the pore water was between 1.22 and 1.32 (Figure 6d). These values indicate that the carbon in the surface and pore waters are terrestrially derived because they are at or above 1.2 (Cory & McKnight, 2005; McKnight et al., 2001).

3.4 | Microbial community composition

While 16S rRNA does not represent metabolism, it is highly conserved for both methanogens and sulfate reducers and is a reliable approximation. Taxa associated with aerobic and anaerobic methane oxidation were found in the soil profile, with taxa associated with aerobic methane oxidation more prevalent near the soil surface (0–25 cm; Figure 7a). Taxa associated with anaerobic methane oxidation pathways were found deeper in the soil profile, increasing to 0.74% at −40 cm before declining with depth. We also found taxa associated with two methanogenesis pathways: hydrogenotrophic and methylotrophic (Figure 7a). Both taxa associated with hydrogenotrophic methanogenesis and with methylotrophic methanogenesis were found in the soil profile. The percentage of taxa associated with hydrogenotrophic methanogenesis increased with depth to 0.77% at −40 cm, before steadily declining to 0.28% at −70 cm. Taxa associated with methylotrophic methanogenesis were found between −20 and −70 cm, with the highest percentage (0.17%) at −65 cm.

We also assessed the percentage of taxa associated with sulfate reduction, which were found in higher percentages than the methanogens and the methanotrophs (Figure 7b). More taxa associated with sulfate reduction were found closer to the soil surface with a peak of 11% at −10 cm. Their abundance dropped from −20 to −70 cm when compared to the near-surface abundances.

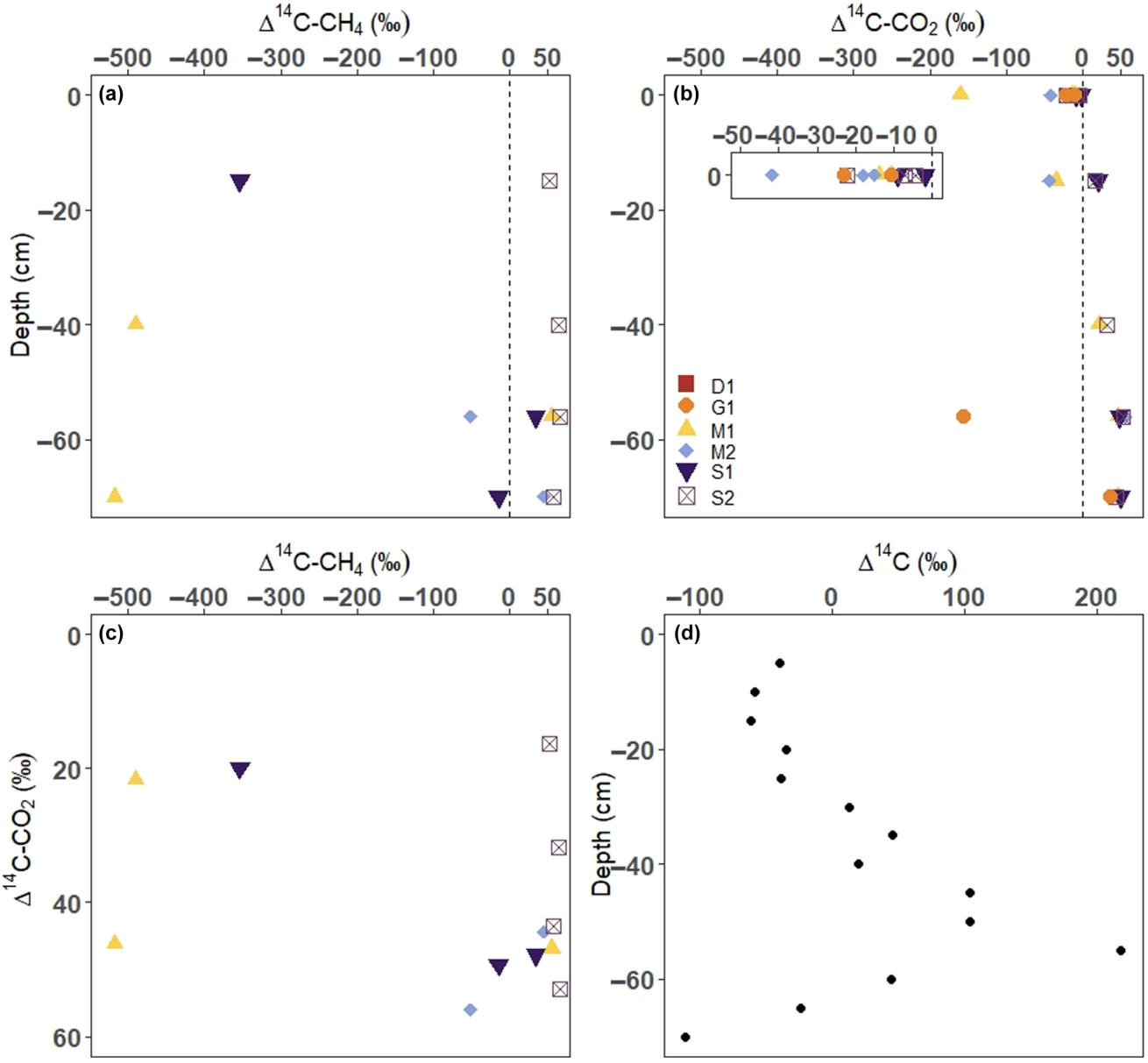

FIGURE 5 Radiocarbon depth profiles of (a) CH_4 and (b) CO_2. Panel (b) also shows the $\Delta^{14}C$-CO_2 of surface soil CO_2 fluxes to the atmosphere which are plotted at 0 cm. Panel (c) shows the relationship between $\Delta^{14}C$-CH_4 and $\Delta^{14}C$-CO_2. Panel (d) shows the age-depth profile of bulk soil $\Delta^{14}C$. Note that not all $\Delta^{14}C$-CO_2 has a corresponding $\Delta^{14}C$-CH_4 because some sampling events did not yield enough CH_4 for radiocarbon analyses.

4 | DISCUSSION

4.1 | CH_4 production within the soil

Our results challenge the current paradigm that assumes that sulfate reduction suppresses CH_4 production in salt marshes. Here, we present unexpectedly high CH_4 concentrations alongside high sulfide concentrations within the soil, demonstrating that CH_4 production (i.e., methanogenesis) co-occurs with sulfate reduction. This finding challenges the assumption that acetoclastic and/or hydrogenotrophic methanogenesis are the primary pathways for CH_4 production in salt marshes. The coexistence of high CH_4 concentrations alongside sulfate reduction, the significant positive relationship between CH_4 concentration and S^{2-} (Figure 2), and the presence of methylotrophic methanogenic taxa in the soil profile provide evidence for the co-occurrence of methylotrophic methanogenesis. Therefore, our results contribute to the growing evidence that salt marsh CH_4 dynamics are more complex than previously thought because multiple methanogenesis pathways coexist that may be difficult to disentangle (Seyfferth et al., 2020; Xiao et al., 2018; Zhuang et al., 2018). This challenge leads to "cryptic CH_4 cycling" where not all fluxes and pathways are currently measured or identified (Krause & Treude, 2021; Xiao et al., 2018), but there is evidence of critical components of important biogeochemical processes as described below.

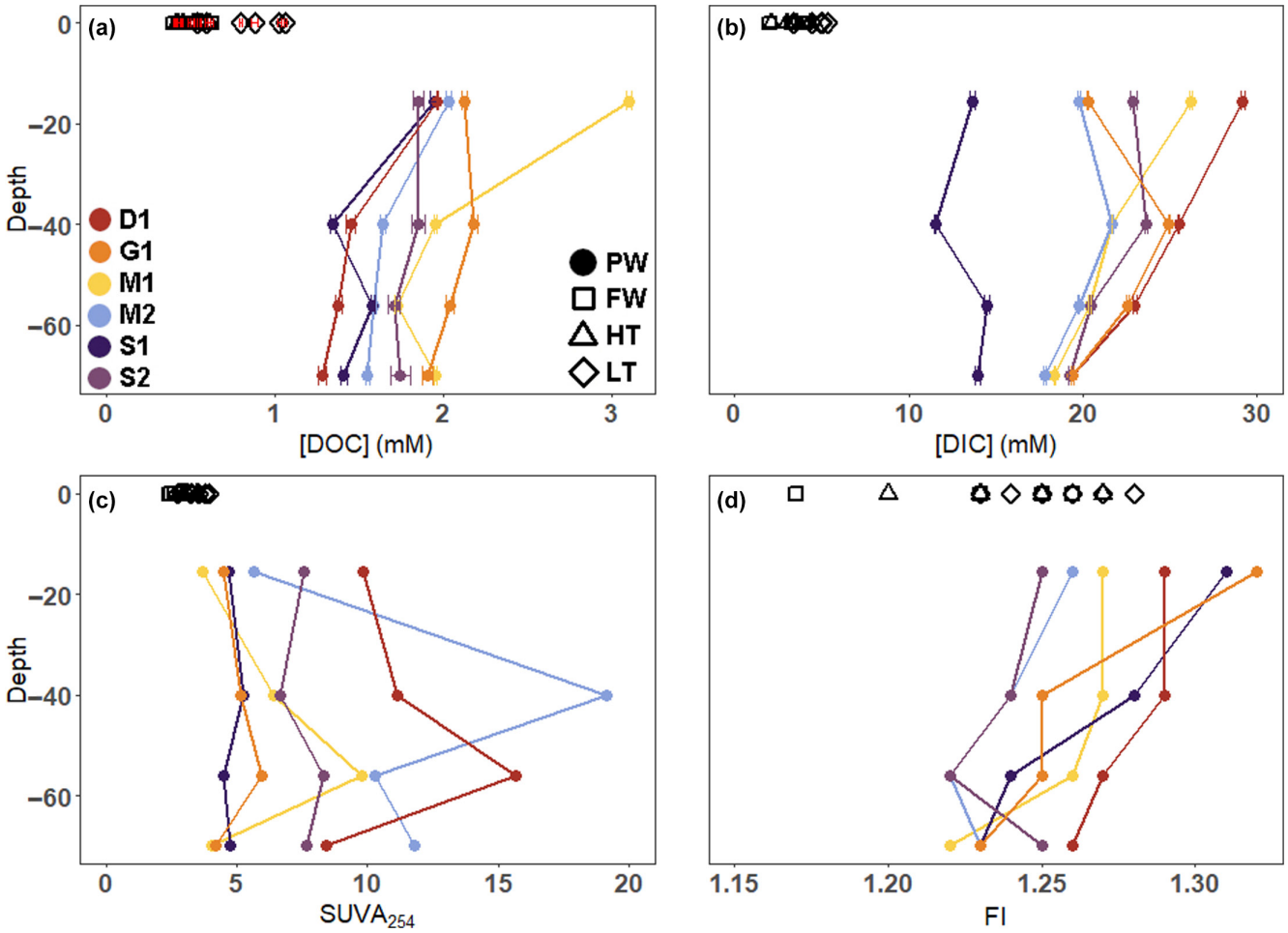

FIGURE 6 Depth profiles and surface water concentrations of (a) DOC, (b) DIC, (c) $SUVA_{254}$, and (d) FI during each of the six campaigns. DIC, dissolved inorganic carbon; DOC, dissolved organic carbon; FI, fluorescence index; FW, freshwater at St. Jones River; HT, creek surface water at high tide; LT, creek surface water at low tide; PW, soil pore water; DOC and DIC standard errors in panels (a, b) represent instrument measurement error.

Two lines of evidence, as discussed in the following paragraphs on the natural abundance of stable isotopes and microbial community composition, point toward two co-occurring methanogenesis pathways at our study site: methylotrophic and hydrogenotrophic. Depth profiles of $\delta^{13}C\text{-}CH_4$ ranged from −68.8‰ to −46.4‰, which falls within isotopic values associated with hydrogenotrophic (−110‰ to −60‰; Whiticar, 1999) and acetoclastic methanogenesis (−70‰ to −50‰; Whiticar, 1999). The range of $\delta^{13}C\text{-}CH_4$ values from methylotrophic methanogenesis within natural settings is uncertain, but laboratory cultures have shown enrichment factors similar to those for hydrogenotrophic methanogenesis (Krzycki et al., 1987; Londry et al., 2008; Penger et al., 2012; Summons et al., 1998). Therefore, isotopic data alone suggest multiple methanogenesis pathways, but is insufficient to parse out the contributions of each pathway to the CH_4 pool.

We identified the presence of taxa associated with methylotrophic and hydrogenotrophic methanogenesis with 16S rRNA sequencing. While these methanogenic taxa were found throughout the soil profile, they generally increased with depth, particularly below −15 cm, where the percentage of taxa associated with sulfate reduction started to decline. The presence of the taxa associated with hydrogenotrophic methanogenesis has been found in coastal wetlands (Sánchez-Carrillo et al., 2021; Xiang et al., 2015; Yuan et al., 2019). However, few studies have assessed the presence of methylotrophic methanogens within soils because they have been thought to be less important than acetoclastic and hydrogenotrophic methanogens (Söllinger & Urich, 2019). The presence of taxa associated with methylotrophic methanogens lends support to the hypothesis that methylotrophic methanogenesis can contribute to high CH_4 production within the soil at our study site (Seyfferth et al., 2020).

While the importance of methylotrophic methanogens to global CH_4 cycling is uncertain (Söllinger & Urich, 2019), these microorganisms play an important role in CH_4 dynamics of *S. alterniflora* salt marshes. *S. alterniflora* contributes substrates (i.e., TMA; Wang & Lee, 1994, 1995) and precursors to substrates (i.e., dimethylsulfoniopropionate, which can be used to produce dimethlysulfide [DMS]; Kiene & Visscher, 1987; Larher et al., 1977) that methylotrophic methanogens can use to produce CH_4. Furthermore, methanol, another non-competitive substrate,

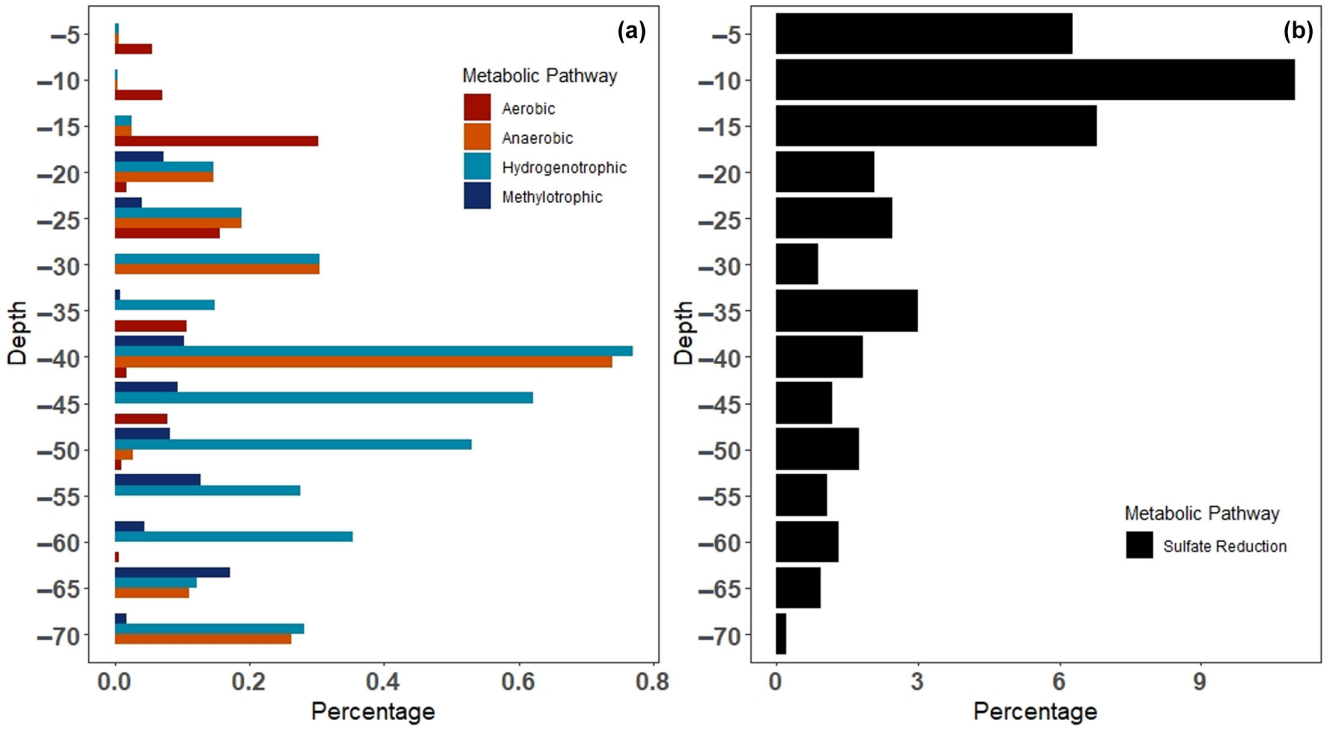

FIGURE 7 Percentage of taxa by depth associated with metabolic pathways. Panel (a) shows methanogenic (hydrogenotrophic, methylotrophic) and methane oxidation (aerobic, anaerobic) pathways, while panel (b) shows taxa typically associated with sulfate reduction.

forms through plant lignin and pectin degradation (Donnelly & Dagley, 1980; Schink & Zeikus, 1980). We highlight that methylotrophic methanogens do not compete with sulfate reducers for substrate, unlike hydrogenotrophic and acetoclastic methanogens (Whiticar, 1999); therefore, methylotrophic methanogens enable high CH_4 production alongside high sulfate reduction. Several studies have shown that *S. alterniflora* invasion resulted in higher levels of CH_4 production (Xiang et al., 2015; Yuan et al., 2016; Zeleke et al., 2013), which has been attributed to an increase in TMA, a non-competitive substrate, and shifts in the dominant methanogen community from either Methanosaetaceae (includes acetoclastic methanogens) or Methanococcales (includes hydrogenotrophic methanogens) to methylotrophic methanogens within Methanosarcinaceae (Yuan et al., 2014, 2016, 2019). Our findings from a native *S. alterniflora* marsh underscore the importance of re-evaluating tidal salt marshes' contribution to CH_4 budgets, particularly for marshes vegetated by species that contribute non-competitive substrates for methanogenesis.

While 16S rRNA identified the presence of taxa associated with methylotrophic and hydrogenotrophic methanogenesis, taxa associated with acetoclastic methanogens were not identified. One reason may be insufficient acetate available for acetoclastic methanogenesis. This finding requires a closer look at the $\delta^{13}C$-CH_4 depth profiles, particularly at −40 cm where the $\delta^{13}C$-CH_4 is isotopically heavier than expected if CH_4 was produced via hydrogenotrophic and/or methylotrophic methanogenesis (Figure S6). One possibility for isotopically heavier CH_4 could be fractionation due to the diffusion of lighter CH_4 toward the soil surface, leaving behind a higher proportion of heavier isotopes. Another possibility is methane oxidation. Concurrent with isotopic enrichment at −40 cm is a peak in the abundance of taxa associated with anaerobic methanotrophs. Studies have highlighted that sulfate-driven anaerobic oxidation of CH_4 likely contributes to some portion of CH_4 oxidation in coastal wetlands (La et al., 2022; Segarra et al., 2013; Wang et al., 2019). While our isotopic and 16S rRNA data suggest that anaerobic CH_4 oxidation occurs at the site, more information regarding substrate availability and microbial activity is needed to identify anaerobic methanotrophs' role in salt marsh soils.

4.2 | Radiocarbon dating of CH_4 and CO_2

Within the soil profile, ^{14}C values for CH_4 are modern, particularly during late senescence, when all four depths had $\Delta^{14}C$-CH_4 >0, indicating that most of this C was fixed from atmospheric CO_2 between 1950 and present. The shift from older (pre-1950) $\Delta^{14}C$-CH_4 values earlier in the growing season to entirely > modern (post 1950) in late senescence corresponds to when both soil and ecosystem CH_4 fluxes are at their highest and most variable at the site (Capooci & Vargas, 2022b; Vázquez-Lule & Vargas, 2021). We postulate that *S. alterniflora* die-off during senescence contributes to increased amounts of labile organic matter and microbial substrates. Research has shown that DMS concentrations in *S. alterniflora* marsh pore waters peaked during plant die-off (Tong et al., 2018). Furthermore, in another *S. alterniflora* marsh, TMA concentrations were eight times higher in the fall than in the summer, corresponding to a nearly

sixfold increase in CH_4 production potential (Yuan et al., 2016). While we did not measure seasonal changes of pore water TMA or DMS concentrations, the increase in soil and ecosystem CH_4 fluxes, as well as the presence of taxa associated with methylotrophic methanogenesis, provides further evidence for CH_4 production via methylotrophic methanogens.

Similar to $\Delta^{14}C\text{-}CH_4$, $\Delta^{14}C\text{-}CO_2$ also followed a general seasonal pattern, becoming slightly heavier during senescence, particularly at −15.5 cm. This likely reflects the input of new labile organic matter and a subsequent increase in the proportion of CO_2 produced from new organic matter versus older organic matter. *S. alterniflora* has been shown to decompose in three phases (Hicks et al., 1991; Lee et al., 1980; Valiela et al., 1985; White & Howes, 1994). The first two phases can contribute to increases in sugars and DOC in the fall (Pakulski, 1986), as well as higher concentrations of biodegradable DOC from senescent material (Shelton et al., 2021; Wang et al., 2014). While soil–atmosphere CO_2 fluxes and belowground concentrations start to decline during senescence, the input of new labile materials likely contributes to young CO_2 in the soil, resulting in an increasingly modern $\Delta^{14}C\text{-}CO_2$. Conversely, the oldest $\Delta^{14}C\text{-}CO_2$ values were generally observed during maturity, suggesting that microbes could access older pools of carbon, likely due to high production rates depleting the easily accessible labile carbon from current growth and the previous senescence. Our findings show that $\Delta^{14}C\text{-}CO_2$ exhibits a seasonality indicative of plant phenology's role in providing substrates for the soil microbial community.

While the depleted $\Delta^{14}C\text{-}CO_2$ could be attributed to seasonal dynamics of older versus newer carbon availability in the soil, there are three older than expected $\Delta^{14}C\text{-}CH_4$ values. These values are older than the surrounding organic matter. Since subsurface gas sampling was from a passive gas sampler that remained in place, the old $\Delta^{14}C\text{-}CH_4$ or the substrate used to produce it likely originated from elsewhere within the marsh, suggesting substantial unmeasured lateral fluxes. Sampling was done in an area where the soil pore waters exchange with creek waters during very high tides, such as after large storm events and during high spring tides (Seyfferth et al., 2020). As a result, the soils become strongly anaerobic, with redox values as low as −200 mV (Seyfferth et al., 2020). Sample collection for $\Delta^{14}C\text{-}CO_2$ and $\Delta^{14}C\text{-}CH_4$ during M1 and S1 occurred 2 days after a storm event and a new moon, respectively, resulting in replenishment of the soil pore water. The mixing of tidal or rainwater with the stagnant pore water establishes hydrological connectivity between less connected pore spaces where old labile C could be physically protected (Franklin et al., 2021; Strong et al., 2004) to more connected pore spaces that have substrates available to process the old C. Furthermore, increased hydrological connectivity due to spring high tide in S1 could contribute to a less reducing environment (Cook et al., 2007) that provides more favorable conditions for oxidizing old carbon, likely leading to the production of old $\Delta^{14}C\text{-}CH_4$. Our measurements of older $\Delta^{14}C\text{-}CH_4$ after spring tides and rain events highlight the importance of better understanding how interactions between hydrological patterns and redox conditions influence salt marsh C dynamics.

4.3 | The complex fate of CH_4

Our results show a large, recently produced soil CH_4 pool with a fast turnover time, suggesting a complex fate for CH_4. CH_4 produced within the soil profile can take many paths, including diffusion into the atmosphere (e.g., Li et al., 2018; Vázquez-Lule & Vargas, 2021), storage within the soil (e.g., Bartlett et al., 1987; Seyfferth et al., 2020), and/or lateral export into adjacent tidal creeks (e.g., Fettrow et al., 2023; Santos et al., 2019; Trifunovic et al., 2020). CH_4 can also be oxidized to CO_2 (e.g., Nielsen et al., 2018; Segarra et al., 2013) or incorporated into the DIC pool and contribute to lateral C export (e.g., La et al., 2022). Plant-mediated transport and ebullition can also be a pathway to support emissions CH_4 into the atmosphere. However, plant-mediated CH_4 transport is highly variable at our study site ranging from negligible to contributing up to 70% of overall soil–atmosphere fluxes (Hill & Vargas, 2022). While detecting ebullition can be difficult, sporadic, instantaneous ebullition events can contribute to a CH_4 pulse that is >2500% higher than the average soil–atmosphere fluxes at the site (Capooci & Vargas, 2022b). Here, we focus our discussion on three fates for CH_4: diffusion into the atmosphere, CH_4 oxidation, and lateral transport to the adjacent tidal creek (Figure 8).

First, soil–atmosphere CH_4 fluxes are generally low and have high variability throughout the year. Daily mean flux during the campaigns ranged from $1.9 \pm 1.1\,\mu mol\,CH_4\,m^{-2}\,day^{-1}$ to $7.28 \pm 59.1\,\mu mol\,CH_4\,m^{-2}\,day^{-1}$. Our measurements fall on the lower end of the range (−93 to >94,000 $\mu mol\,CH_4\,m^{-2}\,day^{-1}$) reported by Al-Haj and Fulweiler (2020). While we found that CH_4 fluxes to the atmosphere increase with increasing soil CH_4 concentration, there are several factors that limit the role of CH_4 fluxes in CH_4 transport. CH_4 diffusion through water-filled pore spaces is slow. Tidal influence at SS is limited to the first few centimeters of the soil; therefore, CH_4 produced in the saturated zone would need to diffuse through water-filled pore spaces to reach the atmosphere. Previous research at the site found that CH_4 fluxes tend to peak during low to rising tides, suggesting that physical forcing contributes to fluxes (Capooci & Vargas, 2022b; Fettrow et al., 2023). Furthermore, CH_4 fluxes were likely impacted by aerobic CH_4 oxidation at the anoxic–oxic interface. Taxa associated with aerobic CH_4 oxidation were found near the soil surface at our site, particularly at −15 cm, and could contribute to the discrepancy between the high CH_4 concentrations at deeper depths and the low fluxes from the soil surface. Thus, the combined effects of slow diffusion rates and the presence of taxa associated with aerobic CH_4 oxidation near the soil surface likely contributed to low CH_4 fluxes from the soil surface, despite high CH_4 production within the soil profile.

Second, we found isotopic and microbial evidence of CH_4 oxidation, but the pathways and definite role of CH_4 oxidation on CH_4 dynamics warrant further study. Our results show that CH_4 oxidation is possible ($\delta^{13}C\text{-}CH_4$ values up to −18‰). Still, it is not a consistently dominant process that could explain the decoupling between high CH_4 concentrations within the soil and relatively low CH_4 fluxes from soils to the atmosphere. During

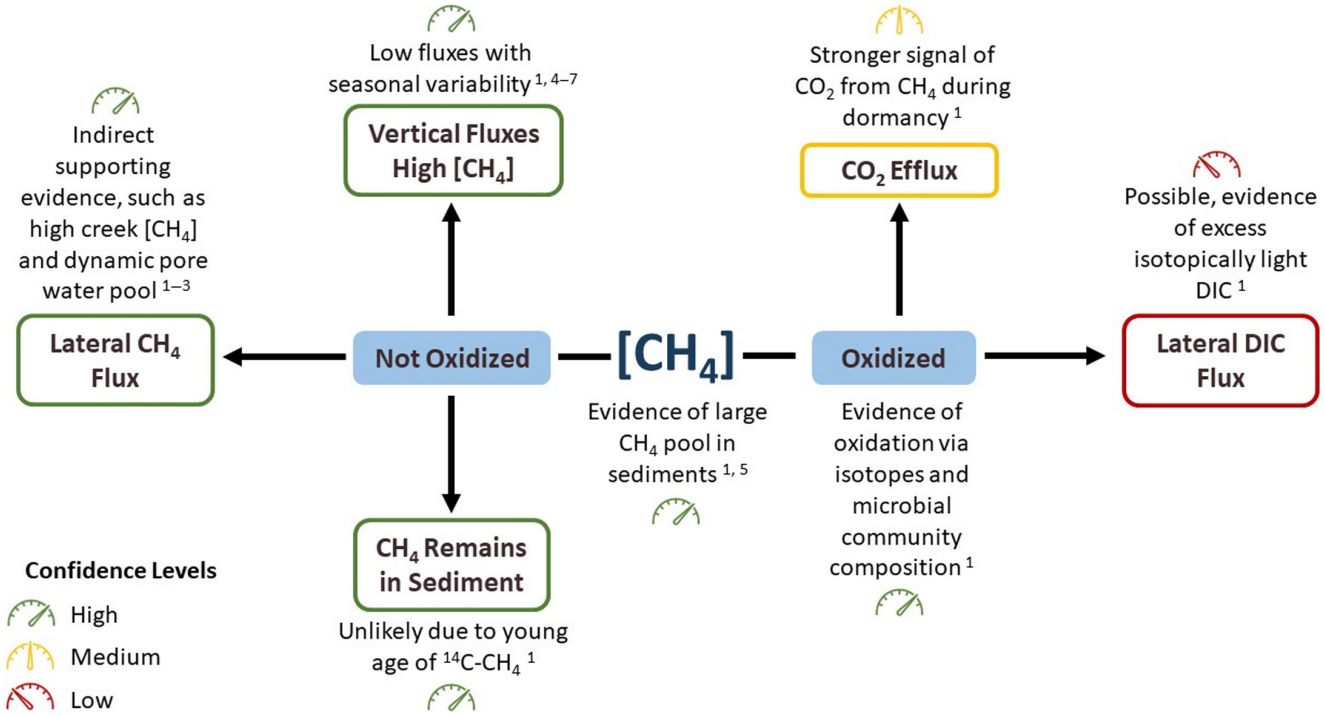

FIGURE 8 Schematic of possible CH_4 pathways and their associated likelihood. Note that all references represent research conducted at the St. Jones Reserve and therefore are tested possibilities for possible CH_4 pathways. *References*: [1]This study; [2]Fettrow et al. (2023); [3]Trifunovic et al. (2020); [4]Capooci and Vargas (2022b); [5]Seyfferth et al. (2020); [6]Vázquez-Lule and Vargas (2021); [7]Hill and Vargas (2022).

CH_4 oxidation, ^{12}C is preferentially oxidized, resulting in the residual CH_4 becoming more enriched in ^{13}C (Barker & Fritz, 1981; Coleman et al., 1981; Silverman & Oyama, 1968). When comparing the mean $\delta^{13}C\text{-}CH_4$ at −15.5 cm to the mean $\delta^{13}C\text{-}CH_4$ of CH_4 flux from the soil surface (−59‰ ± 5‰ vs. −48‰ ± 14‰), we find that, on average, CH_4 fluxes are 11‰ ± 16‰ isotopically heavier compared to CH_4 at −15.5 cm. This isotopic difference is comparable to sedimentary CH_4 and CH_4 fluxes from a swamp forest (Happell et al., 1994). When plotting the $\delta^{13}C\text{-}CH_4$ versus $\delta D\text{-}CH_4$ for data collected in July 2021 (Figure S7; Supplementary Text S1), there is a trend toward CH_4 oxidation as $\delta D\text{-}CH_4$ values become heavier (Whiticar, 1999). Furthermore, we found the presence of taxa associated with aerobic CH_4 oxidation in the top 15 cm of the soil, indicating that some proportion of CH_4 is likely aerobically oxidized at the anoxic–oxic interface. Aerobic methanotrophs have been found near the soil surface in several coastal brackish marshes (McDonald et al., 2005; Moussard et al., 2009; Steinle et al., 2017) and have been shown to have the highest oxidation potential at the anoxic–oxic interface due to the presence of O_2 within the oxic zone and the diffusion of CH_4 from the anoxic zone (Amaral & Knowles, 1994; Buchholz et al., 1995; King, 1990, 1994; Segers, 1998).

The heaviest soil–atmosphere $\delta^{13}C\text{-}CH_4$ fluxes occurred during D1 and G1, indicating that the proportion of CH_4 oxidation is higher during the winter and the early growing season. The CH_4 oxidation signal in these fluxes is likely due to aerobic CH_4 oxidation near the soil surface. Aerobic methanotrophs are less sensitive to temperature than methanogens (Q_{10} of 1.9 vs. 4.1; Segers, 1998) and can oxidize CH_4 in temperatures ranging from −1 to 30°C (King & Adamsen, 1992). Subsequently, the rate of CH_4 production decreases more drastically than the rate of CH_4 oxidation in soils, thereby shifting the balance of the two processes toward oxidation in cooler months. Furthermore, water can hold more oxygen when temperatures are cooler, potentially contributing to increased CH_4 oxidation in the winter. As a result, soil–atmosphere $\delta^{13}C\text{-}CH_4$ fluxes more clearly demonstrate the presence of CH_4 oxidation during D1 and G1 than during periods where high CH_4 production can obscure the presence of CH_4 oxidation. At high CH_4 concentrations, the isotopic shift due to CH_4 oxidation is more difficult to detect (Whiticar & Faber, 1986), mainly because the fractionation factors associated with aerobic CH_4 oxidation are smaller than those for hydrogenotrophic methanogenesis (Happell et al., 1994; Preuss et al., 2013; Whiticar & Faber, 1986). Therefore, using natural abundance isotopes to discern the occurrence of CH_4 oxidation within these soils requires more targeted approaches such as inhibition experiments, tracer experiments, and microbial activity measurements to elucidate the role of CH_4 oxidation in CH_4 dynamics.

While the $\delta^{13}C\text{-}CH_4$ flux data showed that CH_4 oxidation could influence potential soil–atmosphere CH_4 emissions, $\delta^{13}C\text{-}CO_2$ data resemble soil CO_2 and DIC isotopic values, which makes it hard to detect the importance of CH_4 oxidation on the CO_2 pool (Supplementary Text S2; Figure S8). Soil CO_2 produced from CH_4 oxidation is isotopically depleted due to microbial preference for ^{12}C (Barker & Fritz, 1981; Coleman et al., 1981; Silverman &

Oyama, 1968), contributing isotopically light CO_2 into the soil CO_2 and DIC pool. However, due to the size of the CO_2 and the DIC pool (of which CO_2 is a part), as well as inputs of DIC from the tidal creek and continual production of CO_2 from organic matter, the isotopic signature from CH_4 oxidation could get obscured (Whiticar & Faber, 1986). That said, several studies have shown that anaerobic CH_4 oxidation may contribute to the DIC pool in coastal wetlands (La et al., 2022) and marine environments (Chen et al., 2010; Haese et al., 2003; Yoshinaga et al., 2014). Furthermore, there is evidence that while anaerobic oxidation of CH_4 contributes upwards of 8.6% to the pore water DIC pool, between 71% and 96% of the CH_4 gets consumed in the process, illustrating that large amounts of anaerobic CH_4 oxidation minimally impacts the DIC pool (La et al., 2022). Our results show that δ^{13}C-DIC has an excess of isotopically light DIC during some periods of the year (Figure S9). Therefore, we postulate that while excess DIC can come from a variety of sources (e.g., organic matter production, plant and microbial respiration, tidal exchange), the high CH_4 concentrations, low CH_4 fluxes, and isotopically heavy δ^{13}C-CH_4 at the site suggest that CH_4 oxidation contributes to the DIC pool.

Third, we found evidence of potential lateral movement of CH_4 produced in the soil into nearby tidal channels. The variability in concentrations and quality of DOC within the creek water and soil pore water indicates that the DOC pool is more terrestrially derived (Cory & McKnight, 2005; McKnight et al., 2001). The high seasonal variability in $SUVA_{254}$ suggests a highly dynamic pore water DOM pool, reflecting dynamic lateral and/or vertical hydrologic inputs from the tidal creek. Previous research showed that the first 10 cm are likely to be influenced by diurnal tidal cycles and therefore are hydrologically connected to the tidal creek (Guimond et al., 2020), while the pore waters below 10 cm experience tidal exchange during spring-neap cycles, likely enabling more microbial processing of DOC and higher $SUVA_{254}$. Furthermore, the CH_4 and CO_2 within the soil are generally recently produced suggesting high turnover and low residence times within the soil. A previous study at the site demonstrated that the tidal channels are supersaturated with CH_4 (up to 6000 $\mu mol\,mol^{-1}$) and represent a hotspot for CH_4 water–atmosphere fluxes (Trifunovic et al., 2020). One potential explanation for the high turnover in the soil pore water and high CH_4 concentrations in the creek is tidal pumping, which is the exchange of pore water in the sediments with the surface water from the creek via tides (Gleeson et al., 2013; Li et al., 2009; Robinson et al., 2007; Santos et al., 2012). Tidal pumping imports substrates into the pore waters and exports biogeochemical reaction products to the tidal creek (Bouillon et al., 2007; Gleeson et al., 2013; Maher et al., 2013; Santos et al., 2021). We postulate that tidal pumping occurs during spring-neap tidal cycles enabling the build-up of reaction products such as CH_4 and DIC. Studies have shown that DIC export via tidal pumping occurs in coastal systems (e.g., Borges & Abril, 2012; Call et al., 2015; Tamborski et al., 2021). This hypothesis is further supported by similar δ^{13}C-CH_4 and δ^{13}C-CO_2 values for both water–atmosphere and soil–atmosphere fluxes (Supplementary Text S2; Table S2). Therefore, we report different lines of evidence to support the importance of hydrologic connectivity to lateral export of CH_4 from sediments to adjacent tidal channels.

5 | CONCLUSION

Through combined concentration, flux, isotopic, pore water and organic carbon chemistry, and microbial community composition data, we identified that CH_4 dynamics within a tidal salt marsh are biogeochemically heterogeneous, with multiple avenues for CH_4 production and fate. Two co-occurring methanogenesis pathways, methylotrophic and hydrogenotrophic, were identified in the marsh. Once produced, CH_4 had several fates, with soil–atmosphere fluxes, methane oxidation, and lateral transport into the tidal creek likely playing key roles in the CH_4 cycle. These pathways and fates likely co-occur and vary in importance over tidal and seasonal cycles. For example, methylotrophic methanogenesis may be more prevalent in the fall, when *S. alterniflora* die-off contributes substrates used by methylotrophic methanogens. We hope that this study motivates future research to quantify the rates, magnitudes, and underlying processes that regulate and contribute to salt marsh CH_4 dynamics to close the carbon budget in these and other tidal wetlands.

AUTHOR CONTRIBUTIONS

Margaret Capooci: Conceptualization; data curation; formal analysis; investigation; methodology; writing – original draft. **Angelia L. Seyfferth:** Conceptualization; methodology; writing – review and editing. **Craig Tobias:** Methodology; writing – review and editing. **Andrew S. Wozniak:** Methodology; writing – review and editing. **Alexandra Hedgpeth:** Investigation; writing – review and editing. **Malique Bowen:** Investigation; writing – review and editing. **Jennifer F. Biddle:** Methodology; writing – review and editing. **Karis J. McFarlane:** Investigation; methodology; writing – review and editing. **Rodrigo Vargas:** Conceptualization; funding acquisition; methodology; project administration; supervision; writing – review and editing.

ACKNOWLEDGMENTS

This research was supported by the National Science Foundation (NSF-1652594) and the US Department of Energy (#DE-SC0023099 and #DE-SC0022185). Margaret Capooci acknowledges support from an NSF Graduate Research Fellowship (NSF-1247394) and the Department of Energy's Office of Science Graduate Student Research Program (DE-SC0014664). A portion of this work was performed under the auspices of the U.S. Department of Energy by Lawrence Livermore National Laboratory under Contract DE-AC52-07NA27344. We thank the onsite support from Kari St. Laurent and the Delaware National Estuarine Research Reserve, as well as from Victor and Evelyn Capooci for field assistance during the first campaign and Sean Fettrow for assistance with soil coring. The authors acknowledge that the land on which they conducted this study is the traditional homeland of the Lenni-Lenape

tribal nation (Delaware nation). Any opinions, findings. and conclusions or recommendations expressed in this material are those of the author(s) and do not necessarily reflect the views of the National Science Foundation.

CONFLICT OF INTEREST STATEMENT

The authors declare no conflict of interest.

DATA AVAILABILITY STATEMENT

The data that support the findings of this study are openly available in Figshare at https://doi.org/10.6084/m9.figshare.24539050.v1 (Capooci et al., 2023).

ORCID

Margaret Capooci https://orcid.org/0000-0002-4320-2345
Angelia L. Seyfferth https://orcid.org/0000-0003-3589-6815
Craig Tobias https://orcid.org/0000-0003-0120-9984
Andrew S. Wozniak https://orcid.org/0000-0002-7079-3144
Jennifer F. Biddle https://orcid.org/0000-0002-4344-8724
Karis J. McFarlane https://orcid.org/0000-0001-6390-7863
Rodrigo Vargas https://orcid.org/0000-0001-6829-5333

REFERENCES

Al-Haj, A. N., & Fulweiler, R. W. (2020). A synthesis of methane emissions from shallow vegetated coastal ecosystems. *Global Change Biology*, *26*, 2988–3005. https://doi.org/10.1111/gcb.15046

Amaral, J. A., & Knowles, R. (1994). Methane metabolism in a temperate swamp. *Applied and Environmental Microbiology*, *60*, 3945–3951. https://doi.org/10.1128/aem.60.11.3945-3951.1994

Barker, J. F., & Fritz, P. (1981). Carbon isotope fractionation during microbial methane oxidation. *Nature*, *293*, 289–291. https://doi.org/10.1038/293289a0

Bartlett, K. B., Bartlett, D. S., Harriss, R. C., & Sebacher, D. I. (1987). Methane emissions along a salt marsh salinity gradient. *Biogeochemistry*, *4*, 183–202. https://doi.org/10.1007/BF02187365

Borges, A. V., & Abril, G. (2012). *Carbon dioxide and methane dynamics in estuaries*. Elsevier, Inc. https://doi.org/10.1016/B978-0-12-374711-2.00504-0

Bouillon, S., Middelburg, J. J., Dehairs, F., Borges, A. V., Abril, G., Flindt, M. R., Ulomi, S., & Kristensen, E. (2007). Importance of intertidal intertidal sediment processes and porewater exchange on the water column biogeochemistry in a pristine mangrove creek (Ras Dege, Tanzania). *Biogeosciences*, *4*, 311–322. https://doi.org/10.5194/bg-4-311-2007

Broek, T. A. B., Ognibene, T. J., McFarlane, K. J., Moreland, K. C., Brown, T. A., & Bench, G. (2021). Conversion of the LLNL/CAMS 1 MV biomedical AMS system to a semi-automated natural abundance ^{14}C spectrometer: System optimization and performance evaluation. *Nuclear Instruments and Methods in Physics Research. Section B, Beam Interactions with Materials and Atoms*, *499*, 124–132. https://doi.org/10.1016/j.nimb.2021.01.022

Buchholz, L. A., Klump, J. V., Collins, M. L. P., Brantner, C. A., & Remsen, C. C. (1995). Activity of methanotrophic bacteria in Green Bay sediments. *FEMS Microbiology Ecology*, *16*, 1–8. https://doi.org/10.1016/0168-6496(94)00063-3

Call, M., Maher, D. T., Santos, I. R., Ruiz-Halpern, S., Mangion, P., Sanders, C. J., Erler, D. V., Oakes, J. M., Rosentreter, J., Murray, R., & Eyre, B. D. (2015). Spatial and temporal variability of carbon dioxide and methane fluxes over semi-diurnal and spring-neap-spring timescales in a mangrove creek. *Geochimica et Cosmochimica Acta*, *150*, 211–225. https://doi.org/10.1016/j.gca.2014.11.023

Capooci, M., Barba, J., Seyfferth, A. L., & Vargas, R. (2019). Experimental influence of storm-surge salinity on soil greenhouse gas emissions from a tidal salt marsh. *Science of the Total Environment*, *686*, 1164–1172. https://doi.org/10.1016/j.scitotenv.2019.06.032

Capooci, M., Seyfferth, A. L., Craig, T., Wozniak, A. S., Hedgpeth, A., Bowen, M., Biddle, J. F., McFarlane, K. J., & Vargas, R. (2023). *Dataset: High methane concentrations in tidal salt marsh soils: Where does the methane go?* Figshare. https://doi.org/10.6084/m9.figshare.24539050.v1

Capooci, M., & Vargas, R. (2022a). Diel and seasonal patterns of soil CO_2 efflux in a temperate tidal marsh. *Science of the Total Environment*, *802*, 149715. https://doi.org/10.1016/j.scitotenv.2021.149715

Capooci, M., & Vargas, R. (2022b). Trace gas fluxes from tidal salt marsh soils: Implications for carbon-sulfur biogeochemistry. *Biogeosciences*, *19*, 4655–4670. https://doi.org/10.5194/bg-19-4655-2022

Chen, Y., Ussler, W., Haflidason, H., Lepland, A., Rise, L., Hovland, M., & Hjelstuen, B. O. (2010). Sources of methane inferred from pore-water $\delta^{13}C$ of dissolved inorganic carbon in Pockmark G11, offshore Mid-Norway. *Chemical Geology*, *275*, 127–138. https://doi.org/10.1016/j.chemgeo.2010.04.013

Chin, Y. P., Alken, G., & O'Loughlin, E. (1994). Molecular weight, polydispersity, and spectroscopic properties of aquatic humic substances. *Environmental Science & Technology*, *28*, 1853–1858. https://doi.org/10.1021/es00060a015

Coleman, D. D., Risatti, J. B., & Schoell, M. (1981). Fractionation of carbon and hydrogen isotopes by methane-oxidizing bacteria. *Geochimica et Cosmochimica Acta*, *45*, 1033–1037. https://doi.org/10.1016/0016-7037(81)90129-0

Cook, P. L. M., Wenzhöfer, F., Glud, R. N., Janssen, F., & Huettel, M. (2007). Benthic solute exchange and carbon mineralization in two shallow subtidal sandy sediments: Effect of advective pore-water exchange. *Limnology and Oceanography*, *52*, 1943–1963. https://doi.org/10.4319/lo.2007.52.5.1943

Cory, R. M., & McKnight, D. M. (2005). Fluorescence spectroscopy reveals ubiquitous presence of oxidized and reduced quinones in dissolved organic matter. *Environmental Science & Technology*, *39*, 8142–8149. https://doi.org/10.1021/es0506962

DNREC. (1999). *Delaware National Estuarine Research Reserve estuarine profile*. Delaware National Estuarine Research Reserve.

Donnelly, M. I., & Dagley, S. (1980). Production of methanol from aromatic acids by *Pseudomonas putida*. *Journal of Bacteriology*, *142*, 916–924.

Fettrow, S., Vargas, R., & Seyfferth, A. L. (2023). Experimentally simulated sea level rise destabilizes carbon-mineral associations in temperate tidal marsh soil. *Biogeochemistry*, *163*, 103–120. https://doi.org/10.1007/s10533-023-01024-z

Filippa, G., Cremonese, E., Migliavacca, M., Galvagno, M., Folker, M., Richardson, A. D., & Tomelleri, E. (2020). *phenopix: Process digital images of a vegetation cover*. R package version 2.4.2.

Franklin, S. M., Kravchenko, A. N., Vargas, R., Vasilas, B., Fuhrmann, J. J., & Jin, Y. (2021). The unexplored role of preferential flow in soil carbon dynamics. *Soil Biology and Biochemistry*, *161*, 108398. https://doi.org/10.1016/J.SOILBIO.2021.108398

Gleeson, J., Santos, I. R., Maher, D. T., & Golsby-Smith, L. (2013). Groundwater-surface water exchange in a mangrove tidal creek: Evidence from natural geochemical tracers and implications for nutrient budgets. *Marine Chemistry*, *156*, 27–37. https://doi.org/10.1016/j.marchem.2013.02.001

Graven, H. D., Guilderson, T. P., & Keeling, R. F. (2012). Observations of radiocarbon in CO_2 at La Jolla, California, USA 1997–2007: Analysis of the long-term trend. *Journal of Geophysical Research: Atmospheres*, *117*, D02302. https://doi.org/10.1029/2011JD016533

Guimond, J. A., Seyfferth, A. L., Moffett, K. B., & Michael, H. A. (2020). A physical-biogeochemical mechanism for negative feedback between marsh crabs and carbon storage. *Environmental Research Letters*, *15*, 9. https://doi.org/10.1088/1748-9326/ab60e2

Haese, R. R., Meile, C., Van Cappellen, P., & De Lange, G. J. (2003). Carbon geochemistry of cold seeps: Methane fluxes and transformation in sediments from Kazan mud volcano, eastern Mediterranean Sea. *Earth and Planetary Science Letters*, *212*, 361–375. https://doi.org/10.1016/S0012-821X(03)00226-7

Happell, J. D., Chanton, J. P., & Showers, W. S. (1994). The influence of methane oxidation on the stable isotopic composition of methane emitted from Florida swamp forests. *Geochimica et Cosmochimica Acta*, *58*, 4377–4388. https://doi.org/10.1016/0016-7037(94)90341-7

Hicks, R. E., Lee, C., & Marinucci, A. C. (1991). Loss and recycling of amino acids and protein from smooth cordgrass (*Spartina alterniflora*) litter. *Estuaries*, *14*, 430–439. https://doi.org/10.2307/1352267

Hill, A. C., & Vargas, R. (2022). Methane and carbon dioxide fluxes in a temperate tidal salt marsh: Comparisons between plot and ecosystem measurements. *Journal of Geophysical Research: Biogeosciences*, *127*, e2022JG006943. https://doi.org/10.1029/2022JG006943

Hill, A. C., Vázquez-Lule, A., & Vargas, R. (2021). Linking vegetation spectral reflectance with ecosystem carbon phenology in a temperate salt marsh. *Agricultural and Forest Meteorology*, *307*, 108481. https://doi.org/10.1016/j.agrformet.2021.108481

Hood, E., Williams, M. W., & McKnight, D. M. (2005). Sources of dissolved organic matter (DOM) in a Rocky Mountain stream using chemical fractionation and stable isotopes. *Biogeochemistry*, *74*, 231–255. https://doi.org/10.1007/s10533-004-4322-5

Kiene, R. P., & Visscher, P. T. (1987). Production and fate of methylated sulfur compounds from methionine and dimethylsulfoniopropionate in anoxic salt marsh sediments. *Applied and Environmental Microbiology*, *53*, 2426–2434.

King, G. M. (1990). Dynamics and controls of methane oxidation in a Danish wetland sediment. *FEMS Microbiology Ecology*, *74*, 309–323. https://doi.org/10.1111/J.1574-6941.1990.TB01698.X

King, G. M. (1994). Associations of methanotrophs with the roots and rhizomes of aquatic vegetation. *Applied and Environmental Microbiology*, *60*, 3220–3227. https://doi.org/10.1128/aem.60.9.3220-3227.1994

King, G. M., & Adamsen, A. P. S. (1992). Effects of temperature on methane consumption in a forest soil and in pure cultures of the methanotroph *Methylomonas rubra*. *Applied and Environmental Microbiology*, *58*, 2758–2763. https://doi.org/10.1128/AEM.58.9.2758-2763.1992

King, G. M., & Wiebe, W. J. (1980). Regulation of sulfate concentrations and methanogenesis in salt marsh soils. *Estuarine and Coastal Marine Science*, *10*, 215–223. https://doi.org/10.1016/S0302-3524(80)80059-4

Kittler, F., Heimann, M., Kolle, O., Zimov, N., Zimov, S., & Göckede, M. (2017). Long-term drainage reduces CO_2 uptake and CH_4 emissions in a Siberian permafrost ecosystem. *Global Biogeochemical Cycles*, *31*, 1704–1717. https://doi.org/10.1002/2017GB005774

Krause, S. J. E., & Treude, T. (2021). Deciphering cryptic methane cycling: Coupling of methylotrophic methanogenesis and anaerobic oxidation of methane in hypersaline coastal wetland sediment. *Geochimica et Cosmochimica Acta*, *302*, 160–174. https://doi.org/10.1016/j.gca.2021.03.021

Krzycki, J. A., Kenealy, W. R., DeNiro, M. J., & Zeikus, J. G. (1987). Stable carbon isotope fractionation by *Methanosarcina barkeri* during methanogenesis from acetate, methanol, or carbon dioxide-hydrogen. *Applied and Environmental Microbiology*, *53*, 2597–2599. https://doi.org/10.1128/aem.53.10.2597-2599.1987

La, W., Han, X., Liu, C. Q., Ding, H., Liu, M., Sun, F., Li, S., & Lang, Y. (2022). Sulfate concentrations affect sulfate reduction pathways and methane consumption in coastal wetlands. *Water Research*, *217*, 118441. https://doi.org/10.1016/j.watres.2022.118441

Larher, F., Hamelin, J., & Stewart, G. R. (1977). L'acide diméthylsulfonium-3 propanoïque de *Spartina anglica*. *Phytochemistry*, *16*, 2019–2020. https://doi.org/10.1016/0031-9422(77)80117-9

Lee, C., Howarth, R. W., & Howes, B. L. (1980). Sterols in decomposing *Spartina alterniflora* and the use of ergosterol in estimating the contribution of fungi to detrital nitrogen. *Limnology and Oceanography*, *25*, 290–303. https://doi.org/10.4319/lo.1980.25.2.0290

Legendre, P. (2018). *lmodel2: Model II regression*. R package version 1.7-3.

Levin, I., & Hesshaimer, V. (2000). Radiocarbon – A unique tracer of global carbon cycle dynamics. *Radiocarbon*, *42*(1), 1145–1155.

Li, H., Dai, S., Ouyang, Z., Xie, X., Guo, H., Gu, C., Xiao, X., Ge, Z., Peng, C., & Zhao, B. (2018). Muti-scale temporal variation of methane flux and its controls in a subtropical tidal salt marsh in eastern China. *Biogeochemistry*, *137*, 163–179. https://doi.org/10.1007/s10533-017-0413-y

Li, X., Hu, B. X., Burnett, W. C., Santos, I. R., & Chanton, J. P. (2009). Submarine ground water discharge driven by tidal pumping in a heterogeneous aquifer. *Ground Water*, *47*, 558–568. https://doi.org/10.1111/j.1745-6584.2009.00563.x

Londry, K. L., Dawson, K. G., Grover, H. D., Summons, R. E., & Bradley, A. S. (2008). Stable carbon isotope fractionation between substrates and products of *Methanosarcina barkeri*. *Organic Geochemistry*, *39*, 608–621. https://doi.org/10.1016/j.orggeochem.2008.03.002

Macreadie, P. I., Costa, M. D. P., Atwood, T. B., Friess, D. A., Kelleway, J. J., Kennedy, H., Lovelock, C. E., Serrano, O., & Duarte, C. M. (2021). Blue carbon as a natural climate solution. *Nature Reviews Earth and Environment*, *2*, 826–839. https://doi.org/10.1038/s43017-021-00224-1

Maher, D. T., Santos, I. R., Golsby-Smith, L., Gleeson, J., & Eyre, B. D. (2013). Groundwater-derived dissolved inorganic and organic carbon exports from a mangrove tidal creek: The missing mangrove carbon sink? *Limnology and Oceanography*, *58*, 475–488. https://doi.org/10.4319/lo.2013.58.2.0475

Manning, M. R., & Melhuish, W. H. (1994). *Atmospheric $\Delta^{14}C$ record from Willington*. Trends: A compendium of data on global change, Carbon Dioxide Information Analysis Center, Oak Ridge National Laboratory, US Department of Energy, Oak Ridge, TN, USA.

McDonald, I. R., Smith, K., & Lidstrom, M. E. (2005). Methanotrophic populations in estuarine sediment from Newport Bay, California. *FEMS Microbiology Letters*, *250*, 287–293. https://doi.org/10.1016/j.femsle.2005.07.016

McKnight, D. M., Boyer, E. W., Westerhoff, P. K., Doran, P. T., Kulbe, T., & Andersen, D. T. (2001). Spectrofluorometric characterization of dissolved organic matter for indication of precursor organic material and aromaticity. *Limnology and Oceanography*, *46*, 38–48. https://doi.org/10.4319/lo.2001.46.1.0038

McNicol, G., Knox, S. H., Guilderson, T. P., Baldocchi, D. D., & Silver, W. L. (2020). Where old meets new: An ecosystem study of methanogenesis in a reflooded agricultural peatland. *Global Change Biology*, *26*, 772–785. https://doi.org/10.1111/gcb.14916

Mer, J., & Le Roger, P. (2001). Production, oxidation, emission and consumption of methane by soils: A review. *European Journal of Soil Biology*, *37*, 25–50.

Miller, M. P., & McKnight, D. M. (2010). Comparison of seasonal changes in fluorescent dissolved organic matter among aquatic lake and stream sites in the Green Lakes Valley. *Journal of Geophysical Research: Atmospheres*, *115*, 985. https://doi.org/10.1029/2009JG000985

Moussard, H., Stralis-Pavese, N., Bodrossy, L., Neufeld, J. D., & Colin Murrell, J. (2009). Identification of active methylotrophic bacteria inhabiting surface sediment of a marine estuary. *Environmental Microbiology Reports*, *1*, 424–433. https://doi.org/10.1111/j.1758-2229.2009.00063.x

Nellemann, C., Corcoran, E., Duarte, C. M., Valdés, L., De Young, C., Fonseca, L., & Grimsditch, G. (2009). *Blue carbon: A rapid*

response assessment. United Nations Environment Programme, GRID-Arendal.

Nielsen, C. S., Hasselquist, N. J., Nilsson, M. B., Öquistm, M., Järveoja, J., & Peichl, M. (2018). A novel approach for high-frequency *in-situ* quantification of methane oxidation in peatlands. *Soil Systems*, *3*(4), 10004. https://doi.org/10.3390/soilsystems3010004

Northrup, K., Capooci, M., & Seyfferth, A. L. (2018). Effects of extreme events on arsenic cycling in salt marshes. *Journal of Geophysical Research: Biogeosciences*, *123*, 1086–1100. https://doi.org/10.1002/2017JG004259

Oikawa, P. Y., Jenerette, G. D., Knox, S. H., Sturtevant, C., Verfaillie, J., Dronova, I., Poindexter, C. M., Eichelmann, E., & Baldocchi, D. D. (2017). Evaluation of a hierarchy of models reveals importance of substrate limitation for predicting carbon dioxide and methane exchange in restored wetlands. *Journal of Geophysical Research: Biogeosciences*, *122*(1), 145–167. https://doi.org10.1002/2016jg003438.

Oremland, R. S., Marsh, L. M., & Polcin, S. (1982). Methane production and simultaneous sulphate reduction in anoxic, salt marsh sediments. *Nature*, *296*, 143–145.

Oreska, M. P. J., McGlathery, K. J., Aoki, L. R., Berger, A. C., Berg, P., & Mullins, L. (2020). The greenhouse gas offset potential from seagrass restoration. *Scientific Reports*, *10*, 1–15. https://doi.org/10.1038/s41598-020-64094-1

Pakulski, J. D. (1986). The release of reducing sugars and dissolved organic carbon from *Spartina alterniflora* Loisel in a Georgia salt marsh. *Estuarine, Coastal and Shelf Science*, *22*, 385–394. https://doi.org/10.1016/0272-7714(86)90063-6

Pataki, D. E., Ehleringer, J. R., Flanagan, L. B., Yakir, D., Bowling, D. R., Still, C. J., Buchmann, N., Kaplan, J. O., Berry, J. A., & Pataki, C. (2003). The application and interpretation of Keeling plots in terrestrial carbon cycle research. *Global Biogeochemical Cycles*, *17*, 1022. https://doi.org/10.1029/2001GB001850

Penger, J., Conrad, R., & Blaser, M. (2012). Stable carbon isotope fractionation by methylotrophic methanogenic archaea. *Applied and Environmental Microbiology*, *78*, 7596–7602. https://doi.org/10.1128/AEM.01773-12/FORMAT/EPUB

Peterson, P. M., Romaschenko, K., Arrieta, Y. H., & Saarela, J. M. (2014). A molecular phylogeny and new subgeneric classification of *Sporobolus* (Poaceae: Chloridoideae: Sporobolinae). *Taxon*, *63*, 1212–1243. https://doi.org/10.12705/636.19

Petrakis, S., Barba, J., Bond-Lamberty, B., & Vargas, R. (2017). Using greenhouse gas fluxes to define soil functional types. *Plant and Soil*, *423*, 285–294. https://doi.org/10.1007/s11104-017-3506-4

Petrakis, S., Seyfferth, A., Kan, J., Inamdar, S., & Vargas, R. (2017). Influence of experimental extreme water pulses on greenhouse gas emissions from soils. *Biogeochemistry*, *133*, 147–164. https://doi.org/10.1007/s10533-017-0320-2

Petrenko, V. V., Smith, A. M., Brailsford, G., Riedel, K., Hua, Q., Lowe, D., Severinghaus, J. P., Levchenko, V., Bromley, T., Moss, R., Mühle, J., & Brook, E. J. (2008). A new method for analyzing ^{14}C of methane in ancient air extracted from glacial ice. *Radiocarbon*, *50*, 53–73. https://doi.org/10.1017/S0033822200043368

Poffenbarger, H. J., Needelman, A., & Megonigal, J. P. (2011). Salinity influence on methane emissions from tidal marshes. *Wetlands*, *31*, 831–842. https://doi.org/10.1007/s13157-011-0197-0

Ponnamperuma, F. N. (1972). The chemistry of submerged soils. *Advances in Agronomy*, *24*, 29–96.

Preuss, I., Knoblauch, C., Gebert, J., & Pfeiffer, E. M. (2013). Improved quantification of microbial CH_4 oxidation efficiency in arctic wetland soils using carbon isotope fractionation. *Biogeosciences*, *10*, 2539–2552. https://doi.org/10.5194/bg-10-2539-2013

Quast, C., Pruesse, E., Yilmaz, P., Gerken, J., Schweer, T., Yarza, P., Peplies, J., & Glöckner, F. O. (2013). The SILVA ribosomal RNA gene database project: Improved data processing and web-based tools. *Nucleic Acids Research*, *41*, D590–D596. https://doi.org/10.1093/NAR/GKS1219

Robinson, C., Li, L., & Prommer, H. (2007). Tide-induced recirculation across the aquifer-ocean interface. *Water Resources Research*, *43*, 5679. https://doi.org/10.1029/2006WR005679

Romera-Castillo, C., Chen, M., Yamashita, Y., & Jaffé, R. (2014). Fluorescence characteristics of size-fractionated dissolved organic matter: Implications for a molecular assembly based structure? *Water Research*, *55*, 40–51. https://doi.org/10.1016/j.watres.2014.02.017

Rosentreter, J. A., Al-Haj, A. N., Fulweiler, R. W., & Williamson, P. (2021). Methane and nitrous oxide emissions complicate coastal blue carbon assessments. *Global Biogeochemical Cycles*, *35*, e2020GB006858. https://doi.org/10.1029/2020GB006858

Rosentreter, J. A., Maher, D. T., Erler, D. V., Murray, R. H., & Eyre, B. D. (2018). Methane emissions partially offset "blue carbon" burial in mangroves. *Science Advances*, *4*, eaao4985. https://doi.org/10.1126/SCIADV.AAO4985

Sánchez-Carrillo, S., Garatuza-Payan, J., Sánchez-Andrés, R., Cervantes, F. J., Bartolomé, M. C., Merino-Ibarra, M., & Thalasso, F. (2021). Methane production and oxidation in mangrove soils assessed by stable isotope mass balances. *Water*, *13*, 31867. https://doi.org/10.3390/w13131867

Söllinger, A., & Urich, T. (2019). Methylotrophic methanogens everywhere – Physiology and ecology of novel players in global methane cycling. *Biochemical Society Transactions*, *47*, 1895–1907. https://doi.org/10.1042/BST20180565

Santos, I. R., Burdige, D. J., Jennerjahn, T. C., Bouillon, S., Cabral, A., Serrano, O., Wernberg, T., Filbee-Dexter, K., Guimond, J. A., & Tamborski, J. J. (2021). The renaissance of Odum's outwelling hypothesis in "blue carbon" science. *Estuarine, Coastal and Shelf Science*, *255*, 107361. https://doi.org/10.1016/j.ecss.2021.107361

Santos, I. R., Eyre, B. D., & Huettel, M. (2012). The driving forces of porewater and groundwater flow in permeable coastal sediments: A review. *Estuarine, Coastal and Shelf Science*, *98*, 1–15. https://doi.org/10.1016/j.ecss.2011.10.024

Santos, I. R., Maher, D. T., Larkin, R., Webb, J. R., & Sanders, C. J. (2019). Carbon outwelling and outgassing vs. burial in an estuarine tidal creek surrounded by mangrove and saltmarsh wetlands. *Limnology and Oceanography*, *64*, 996–1013. https://doi.org/10.1002/lno.11090

Saunois, M., Stavert, A. R., Poulter, B., Bousquet, P., Canadell, J. G., Jackson, R. B., Raymond, P. A., Dlugokencky, E. J., Houweling, S., Patra, P. K., Ciais, P., Arora, V. K., Bastviken, D., Bergamaschi, P., Blake, D. R., Brailsford, G., Bruhwiler, L., Carlson, K. M., Carrol, M., … Zhuang, Q. (2020). The global methane budget 2000–2017. *Earth System Science Data*, *12*, 1561–1623. https://doi.org/10.5194/essd-12-1561-2020

Schink, B., & Zeikus, J. G. (1980). Microbial methanol formation: A major end product of pectin metabolism. *Current Microbiology*, *4*, 387–389. https://doi.org/10.1007/BF02605383

Schloss, P. D., Westcott, S. L., Ryabin, T., Hall, J. R., Hartmann, M., Hollister, E. B., Lesniewski, R. A., Oakley, B. B., Parks, D. H., Robinson, C. J., Sahl, J. W., Stres, B., Thallinger, G. G., Van Horn, D. J., & Weber, C. F. (2009). Introducing mothur: Open-source, platform-independent, community-supported software for describing and comparing microbial communities. *Applied and Environmental Microbiology*, *75*, 7537–7541. https://doi.org/10.1128/AEM.01541-09

Schuur, E. A. G., Trumbore, S. E., Druffel, E. R. M., Southon, J. R., Steinhof, A., Taylor, R. E., & Turnbull, J. C. (2016). Radiocarbon and the global carbon cycle. In E. A. G. Schuur, E. R. M. Druffel, & S. Trumbore (Eds.), *Radiocarbon and climate change* (pp. 1–19). Springer. https://doi.org/10.1007/978-3-319-25643-6_1

Segarra, K. E. A., Samarkin, V., King, E., Meile, C., & Joye, S. B. (2013). Seasonal variations of methane fluxes from an unvegetated tidal

freshwater mudflat (Hammersmith Creek, GA). *Biogeochemistry*, *115*, 349–361. https://doi.org/10.1007/s10533-013-9840-6

Segers, R. (1998). Methane production and methane consumption: A review of processes underlying wetland methane fluxes. *Biogeochemistry*, *41*, 23–51.

Seyfferth, A. L., Bothfeld, F., Vargas, R., Stuckey, J. W., Wang, J., Kearns, K., Michael, H. A., Guimond, J., Yu, X., & Sparks, D. L. (2020). Spatial and temporal heterogeneity of geochemical controls on carbon cycling in a tidal salt marsh. *Geochimica et Cosmochimica Acta*, *282*, 1–18. https://doi.org/10.1016/j.gca.2020.05.013

Sharp, J. H. (2002). Analytical methods for Total DOM pools. In D. A. Hansell & C. A. Carlson (Eds.), *Biogeochemistry of marine dissolved organic matter* (pp. 35–58). Elsevier Science.

Shelton, S., Neale, P., Pinsonneault, A., & Tzortziou, M. (2021). Biodegradation and photodegradation of vegetation-derived dissolved organic matter in tidal marsh ecosystems. *Estuaries and Coasts*, *45*, 1324–1342. https://doi.org/10.1007/s12237-021-00982-7

Silverman, M. P., & Oyama, V. I. (1968). Automatic apparatus for sampling and preparing gases for mass spectral analysis in studies of carbon isotope fractionation during methane metabolism. *Analytical Chemistry*, *40*, 1833–1837.

Steinle, L., Maltby, J., Treude, T., Kock, A., Bange, H. W., Engbersen, N., Zopfi, J., Lehmann, M. F., & Niemann, H. (2017). Effects of low oxygen concentrations on aerobic methane oxidation in seasonally hypoxic coastal waters. *Biogeosciences*, *14*, 1631–1645. https://doi.org/10.5194/bg-14-1631-2017

Strong, D. T., De Wever, H., Merckx, R., & Recous, S. (2004). Spatial location of carbon decomposition in the soil pore system. *European Journal of Soil Science*, *55*, 739–750. https://doi.org/10.1111/j.1365-2389.2004.00639.x

Stuiver, M., & Polach, H. A. (1977). Discussion: Reporting of ^{14}C data. *Radiocarbon*, *19*, 355–363.

Summons, R. E., Franzmann, P. D., & Nichols, P. D. (1998). Carbon isotopic fractionation associated with methylotrophic methanogenesis. *Organic Geochemistry*, *28*, 465–475. https://doi.org/10.1016/S0146-6380(98)00011-4

Taillardat, P., Thompson, B. S., Garneau, M., Trottier, K., & Friess, D. A. (2020). Climate change mitigation potential of wetlands and the cost-effectiveness of their restoration. *Interface Focus*, *10*, 20190129. https://doi.org/10.1098/rsfs.2019.0129

Tamborski, J. J., Eagle, M., Kurylyk, B. L., Kroeger, K. D., Wang, Z. A., Henderson, P., & Charette, M. A. (2021). Pore water exchange-driven inorganic carbon export from intertidal salt marshes. *Limnology and Oceanography*, *66*, 1774–1792. https://doi.org/10.1002/LNO.11721

Tong, C., Morris, J. T., Huang, J., Xu, H., & Wan, S. (2018). Changes in pore-water chemistry and methane emission following the invasion of *Spartina alterniflora* into an oligohaline marsh. *Limnology and Oceanography*, *63*, 384–396. https://doi.org/10.1002/lno.10637

Trifunovic, B., Vázquez-Lule, A., Capooci, M., Seyfferth, A. L., Moffat, C., & Vargas, R. (2020). Carbon dioxide and methane emissions from temperate salt marsh tidal creek. *Journal of Geophysical Research: Biogeosciences*, *125*, 5558. https://doi.org/10.1029/2019JG005558

Trumbore, S. E., Sierra, C. A., & Hicks Pries, C. E. (2016). Radiocarbon nomenclature, theory, models, and interpretation: Measuring age, determining cycling rates, and tracing source pools. In E. A. G. Schuur, E. R. M. Druffel, & S. Trumbore (Eds.), *Radiocarbon and climate change* (pp. 45–82). Springer. https://doi.org/10.1007/978-3-319-25643-6_3

Valiela, I., Teal, J. M., Allen, S. D., Van Etten, R., Goehringer, D., & Volkmann, S. (1985). Decomposition in salt marsh ecosystems: The phases and major factors affecting disappearance of above-ground organic matter. *Journal of Experimental Marine Biology and Ecology*, *89*, 29–54. https://doi.org/10.1016/0022-0981(85)90080-2

Vázquez-Lule, A., & Vargas, R. (2021). Biophysical drivers of net ecosystem and methane exchange across phenological phases in a tidal salt marsh. *Agricultural and Forest Meteorology*, *300*, 108309. https://doi.org/10.1016/j.agrformet.2020.108309

Vogel, J. S., Southon, J. R., Nelson, D. E., & Brown, T. A. (1984). Performance of catalytically condensed carbon for use in accelerator mass spectrometry. *Nuclear Instruments and Methods in Physics Research Section B*, *B5*, 289–293. https://doi.org/10.1016/0168-583X(84)90529-9

Wang, J., Hua, M., Cai, C., Hu, J., Wang, J., Yang, H., Ma, F., Qian, H., Zheng, P., & Hua, B. (2019). Spatial-temporal pattern of sulfate-dependent anaerobic methane oxidation in an intertidal zone of the east China sea. *Applied and Environmental Microbiology*, *85*, e02638-18. https://doi.org/10.1128/AEM.02638-18

Wang, X., Chen, R. F., Cable, J. E., & Cherrier, J. (2014). Leaching and microbial degradation of dissolved organic matter from salt marsh plants and seagrasses. *Aquatic Sciences*, *76*, 595–609. https://doi.org/10.1007/s00027-014-0357-4

Wang, X. C., & Lee, C. (1994). Sources and distribution of aliphatic amines in salt marsh sediment. *Organic Geochemistry*, *22*, 1005–1021. https://doi.org/10.1016/0146-6380(94)90034-5

Wang, X. C., & Lee, C. (1995). Decomposition of aliphatic amines and amino acids in anoxic salt marsh sediment. *Geochimica et Cosmochimica Acta*, *59*, 1787–1797. https://doi.org/10.1016/0016-7037(95)00082-B

Ward, N., Megonigal, P. J., Bond-Lamberty, B., Bailey, V., Butman, D., Canuel, E., Diefenderfer, H., Ganju, N. K., Goñi, M. A., Graham, E. B., Hopkinson, C. S., Khangaonkar, T., Langley, J. A., McDowell, N. G., Myers-Pigg, A. N., Neumann, R. B., Osburn, C. L., Price, R. M., Rowland, J., … Windham-Myers, L. (2020). Representing the function and sensitivity of coastal interfaces in earth system models. *Nature Communications*, *11*, 2458. https://doi.org/10.1038/s41467-020-16236-2

Weishaar, J. L., Aiken, G. R., Bergamaschi, B. A., Fram, M. S., Fujii, R., & Mopper, K. (2003). Evaluation of specific ultraviolet absorbance as an indicator of the chemical composition and reactivity of dissolved organic carbon. *Environmental Science & Technology*, *37*, 4702–4708. https://doi.org/10.1021/es030360x

White, D. S., & Howes, B. L. (1994). Long-term ^{15}N-nitrogen retention in the vegetated sediments of a New England salt marsh. *Limnology and Oceanography*, *39*, 1878–1892. https://doi.org/10.4319/lo.1994.39.8.1878

Whiticar, M. J. (1999). Carbon and hydrogen isotope systematics of bacterial formation and oxidation of methane. *Chemical Geology*, *161*, 291–314. https://doi.org/10.1016/S0009-2541(99)00092-3

Whiticar, M. J., & Faber, E. (1986). Methane oxidation in sediment and water column environments – Isotope evidence. *Organic Geochemistry*, *10*, 759–768. https://doi.org/10.1016/S0146-6380(86)80013-4

Windham-Myers, L., Holmquist, J. R., Kroeger, K. D., & Troxler, T. G. (2022). Greenhouse gas balances in coastal ecosystems: Current challenges in "blue carbon" estimation and significance to national greenhouse gas inventories. In B. Poulter, J. Canadell, D. Hayes, & R. Thompson (Eds.), *Balancing greenhouse gas budgets: Accounting for natural and anthropogenic flows of CO_2 and other trace gases* (pp. 403–425). Elsevier. https://doi.org/10.1016/B978-0-12-814952-2.00001-0

Xiang, J., Liu, D., Ding, W., Yuan, J., & Lin, Y. (2015). Invasion chronosequence of *Spartina alterniflora* on methane emission and organic carbon sequestration in a coastal salt marsh. *Atmospheric Environment*, *112*, 72–80. https://doi.org/10.1016/j.atmosenv.2015.04.035

Xiao, K. Q., Beulig, F., Røy, H., Jørgensen, B. B., & Risgaard-Petersen, N. (2018). Methylotrophic methanogenesis fuels cryptic methane cycling in marine surface sediment. *Limnology and Oceanography*, *63*, 1519–1527. https://doi.org/10.1002/lno.10788

Yoshinaga, M. Y., Holler, T., Goldhammer, T., Wegener, G., Pohlman, J. W., Brunner, B., Kuypers, M. M. M., Hinrichs, K. U., & Elvert, M. (2014). Carbon isotope equilibration during sulphate-limited anaerobic oxidation of methane. *Nature Geoscience*, *7*, 190–194. https://doi.org/10.1038/ngeo2069

Yuan, J., Ding, W., Liu, D., Kang, H., Xiang, J., & Lin, Y. (2016). Shifts in methanogen community structure and function across a coastal marsh transect: Effects of exotic *Spartina alterniflora* invasion. *Scientific Reports*, *6*, 18777. https://doi.org/10.1038/srep18777

Yuan, J., Ding, W., Liu, D., Xiang, J., & Lin, Y. (2014). Methane production potential and methanogenic archaea community dynamics along the *Spartina alterniflora* invasion chronosequence in a coastal salt marsh. *Applied Microbiology and Biotechnology*, *98*, 1817–1829. https://doi.org/10.1007/s00253-013-5104-6

Yuan, J., Liu, D., Ji, Y., Xiang, J., Lin, Y., Wu, M., & Ding, W. (2019). *Spartina alterniflora* invasion drastically increases methane production potential by shifting methanogenesis from hydrogenotrophic to methylotrophic pathway in a coastal marsh. *Journal of Ecology*, *107*, 2436–2450. https://doi.org/10.1111/1365-2745.13164

Zeleke, J., Sheng, Q., Wang, J. G., Huang, M. Y., Xia, F., Wu, J. H., & Quan, Z. X. (2013). Effects of *Spartina alterniflora* invasion on the communities of methanogens and sulfate-reducing bacteria in estuarine marsh sediments. *Frontiers in Microbiology*, *4*, 243. https://doi.org/10.3389/fmicb.2013.00243

Zhang, Y., Li, C., Trettin, C. C., Li, H., & Sun, G. (2002). An integrated model of soil, hydrology, and vegetation for carbon dynamics in wetland ecosystems. *Global Biogeochemical Cycles*, *16*, 1–17. https://doi.org/10.1029/2001GB001838

Zhuang, G.-C., Heuer, V. B., Lazar, C. S., Goldhammer, T., Wendt, J., Samarkin, V. A., Elvert, M., Teske, A. P., Joye, S. B., & Hinrichs, K.-U. (2018). Relative importance of methylotrophic methanogenesis in sediments of the Western Mediterranean Sea. *Geochimica et Cosmochimica Acta*, *224*, 171–186. https://doi.org/10.1016/j.gca.2017.12.024

SUPPORTING INFORMATION

Additional supporting information can be found online in the Supporting Information section at the end of this article.

How to cite this article: Capooci, M., Seyfferth, A. L., Tobias, C., Wozniak, A. S., Hedgpeth, A., Bowen, M., Biddle, J. F., McFarlane, K. J., & Vargas, R. (2023). High methane concentrations in tidal salt marsh soils: Where does the methane go? *Global Change Biology*, *30*, e17050. https://doi.org/10.1111/gcb.17050